

Four loop renormalization of 3-quark operators in QCD

J.A. Gracey,
Theoretical Physics Division,
Department of Mathematical Sciences,
University of Liverpool,
P.O. Box 147,
Liverpool,
L69 3BX,
United Kingdom.

Abstract. We renormalize generalized 3-quark operators that relate to baryon states using the method devised by Kränkl and Manashov at four loops in the $\overline{\text{MS}}$ scheme. The anomalous dimensions of the four core operators used to compute nucleon matrix elements are determined and their associated critical exponents are studied in the conformal window using the Banks-Zaks expansion.

arXiv:2510.21940v2 [hep-ph] 6 Feb 2026

1 Introduction.

It has been long-established that quarks are the fundamental quanta that bind together to form mesons and baryons. Protons and neutrons for instance are comprised of up and down quarks with a wealth of other observed particles built out of the more massive quarks as well as valence gluons. One way to understand the internal structure and properties of protons, for example, requires colliding beams of protons or electrons with other protons. This allows us to quantify the theory models of the constituent quarks which are encapsulated in structure functions or parton distribution functions. The latter are probability distributions of the valence quarks within, say, a proton which if known accurately enough allows one to deduce which partons dominate proton properties such as its overall motion, spin or charge. Moreover having as refined a knowledge as possible of structure functions and distributions is important for making precise theoretical predictions for strong effect background radiation for colliders searching for physics beyond the Standard Model. Theoretically structure functions can only be computed with nonperturbative field theory methods using Quantum Chromodynamics (QCD) as it describes the strong sector. Central to such activities in particular is lattice field theory which requires the use of high performance computing facilities. Improvements in this infrastructure in recent years has led to progress to the extent that operator matrix element evaluation, required for structure functions, has been significantly refined. Included in this overall vision of the theory connection to experiment is a parallel approach which is the use of distribution amplitudes that are also purely nonperturbative quantities. These have focused in recent years on the structure of baryons in several different set-up configurations. See, for instance, [1, 2, 3, 4, 5, 6, 7] for a variety of developments in this area primarily using lattice field theory. In measuring such matrix elements and amplitudes on the lattice, which involve baryon operator Green's functions, the renormalization group running of the operators themselves also plays an important role. In other words the anomalous dimension of the operators are required with the observation that if as much high loop order information as is computationally possible is available then the uncertainties in the extrapolation to the continuum as well as the evolution to low energies can be minimized.

Such continuum high loop order operator renormalization has been carried out for many years for quark bilinear operators such as the twist-2 Wilson operators that describe deep inelastic scattering. These are central to the operator product expansion which is the main tool to probe properties of the proton via its structure functions. However for the distribution amplitude approach the renormalization of baryon operators is a key ingredient for the overall research programme. The renormalization of such operators in purely $SU(3)$ gauge theories has not received as much attention. For instance, the one loop modified minimal subtraction ($\overline{\text{MS}}$) scheme renormalization was carried out in [8, 9, 10] followed by the two loop extension in [11] for proton and neutron related operators. In more recent years with interest extending beyond these two states a general 3-quark operator was renormalized at two loops in [12]. The major benefit of computing the general operator anomalous dimension is that the dimensions of baryon states other than the proton and neutron can be deduced as a corollary. Subsequently the work of [11, 12] was extended to three loops in [13]. With the progress in distribution function analyses the higher order perturbative computation moved in several directions. To assist with lattice matching not only does the programme require the operator anomalous dimensions but the loop expansion of pertinent Green's functions is also necessary. For instance, these Green's functions involve the insertion of a 3-quark operator into a quark 3-point function. Such operator matrix element evaluation was partly addressed in [13] where the 3-quark operator was inserted at zero momentum in a quark 3-point function with the squared momenta of the three external quark legs held at the same value corresponding to a pseudo-symmetric configuration. However, in order to probe proton structure further non-zero momentum operator insertion configurations are needed and this was addressed perturbatively in [14] to two

loops. In that work the 3-quark operator was inserted with a non-zero external momentum where the momenta of the other three quark legs comprising the Green's function of interest were not nullified either. This configuration is more accommodating for lattice measurements especially since the setup was completely symmetric. By this we mean the square of each of the four external momenta were equal. More recently a new phase of 3-quark operator renormalization and Green's function evaluation has opened when the first moment of the 3-quark operators was considered at two loops in [7]. So it is clear there is a well-defined programme of research that is needed to support and complement lattice matching activities for distribution amplitudes.

Such perturbative calculations beyond the lowest loop order are not straightforward. Aside from the large number of Feynman graphs to be evaluated, in order to determine the relevant 3-quark operator Green's functions requires decomposing them into a basis of Lorentz tensors. For any such Green's function the basis is very large and each associated form factor needs to be fully found explicitly perturbatively to be of any benefit for a lattice measurement. This article aims to address one aspect of the 3-quark operator programme by determining the anomalous dimension of the general operator introduced in [12] to four loops in the $\overline{\text{MS}}$ scheme. Consequently we will deduce the anomalous dimensions of various baryon states to the same order. To achieve this level of loop order we make extensive use of the FORCER algorithm, [15, 16], written in the symbolic manipulation language FORM, [17, 18]. The FORCER package is the state of the art tool for extracting divergences from the Green's function configuration we have chosen for the renormalization of the general 3-quark operator to four loops. Since baryon operators have been of recent interest for probing various ideas into beyond the Standard Model physics, (see for instance [19, 20, 21, 22, 23, 24, 25]), we will use our results to study the behaviour of the various baryon operator dimensions in the conformal window. This is achieved through the Banks-Zaks perturbative approach of expanding around a non-trivial zero of the β -function in this window, [26]. Interestingly we were able to re-sum the critical exponents of several operators deep into the lower part of the window. By providing benchmark values of the exponents for various values of N_f , which is the number of quark flavours, it would be interesting to see if these tally with values computed by other techniques such as lattice field theory.

The article is organized as follows. Section 2 is devoted to the background of the general 3-quark operator we will renormalize to four loops including the computational strategy and the technicalities of the generalized γ algebra that is employed. The main results of the renormalization are recorded in Section 3 where the anomalous dimensions of four core baryon operators are deduced from the general 3-quark operator anomalous dimension. The properties of the four baryon operators at the Banks-Zaks critical point are discussed in Section 4 before we present concluding remarks in Section 5. Appendix A records various γ matrix identities which were necessary to translate the operator renormalization constant to the anomalous dimension.

2 General operator

We begin by discussing the renormalization of a general $SU(3)$ gauge invariant 3-quark operator which is, [12],

$$\mathcal{O}_{\alpha\beta\gamma}^{ijk} = \epsilon^{IJK} \psi_{\alpha}^{iI} \psi_{\beta}^{jJ} \psi_{\gamma}^{kK} \quad (2.1)$$

where throughout the quarks are massless, i, j and k are flavour indices and the $SU(3)$ group generators are T_{IJ}^a with $1 \leq a \leq 8$ and $1 \leq I \leq 3$. At the initial stage this general form for the quark content of a baryon operator is renormalized using the same approach as [12] since the anomalous dimensions of specific baryon operators are deduced from an appropriate choice of a γ matrix basis. In order to exploit the efficient four loop FORCER package, [15, 16], written in the

symbolic manipulation language FORM [17, 18] we will evaluate the Green's function

$$G_{(\alpha'\beta'\gamma'|\alpha\beta\gamma)}^{(i'j'k'|ijk)}(p) = \langle \psi_{\alpha'}^{i'}(p) \psi_{\beta'}^{j'}(-p) \psi_{\gamma'}^{k'}(0) \mathcal{O}_{\alpha\beta\gamma}^{ijk}(0) \rangle \quad (2.2)$$

in dimensional regularization in $d = 4 - 2\epsilon$ dimensions where an external momentum flows in one quark leg and out through another. There is no momenta flow through the remaining quark leg or the operator itself. The setup is illustrated graphically in Figure 1. With quark fields only, and no anti-quarks, flowing into the operator insertion then closed quark loops will only occur on internal gluons. An overall flavour tensor can be factored off $G_{(\alpha'\beta'\gamma'|\alpha\beta\gamma)}^{(i'j'k'|ijk)}(p)$ via

$$G_{(\alpha'\beta'\gamma'|\alpha\beta\gamma)}^{(i'j'k'|ijk)}(p) = \mathcal{T}^{(i'j'k'|ijk)} G_{(\alpha'\beta'\gamma'|\alpha\beta\gamma)}(p) \quad (2.3)$$

where

$$\mathcal{T}^{(i'j'k'|ijk)} = \delta^{ii'} \delta^{jj'} \delta^{kk'} + \delta^{ii'} \delta^{jk'} \delta^{kj'} + \delta^{ij'} \delta^{ji'} \delta^{kk'} + \delta^{ij'} \delta^{jk'} \delta^{ki'} + \delta^{ik'} \delta^{ji'} \delta^{kj'} + \delta^{ik'} \delta^{jj'} \delta^{ki'} . \quad (2.4)$$

The structure that remains, $G_{(\alpha'\beta'\gamma'|\alpha\beta\gamma)}(p)$, will involve the tensor product of three strings of γ matrices with open spinor indices. Before the evaluation of an individual Feynman graph each of the strings will have contracted Lorentz indices across the strings as well as contractions with the internal loop momenta. Since the computation was for a fixed colour group $SU(3)$ we made extensive use of the $SU(N_c)$ identity

$$T_{IJ}^a T_{KL}^a = \frac{1}{2} \left[\delta_{IL} \delta_{KJ} - \frac{1}{N_c} \delta_{IJ} \delta_{KL} \right] \quad (2.5)$$

for $N_c = 3$ after using the Lie algebra

$$[T^a, T^b] = i f^{abc} T^c \quad (2.6)$$

to replace any structure functions f^{abc} that arise from the gluon and ghost vertex Feynman rules.

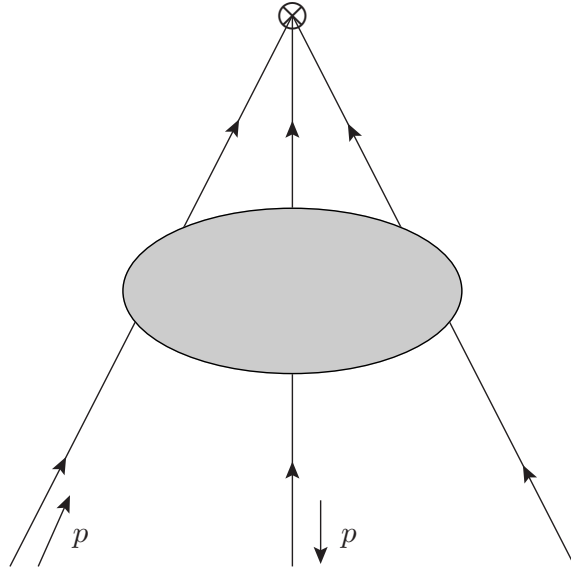


Figure 1: Graphical structure of the Green's function $G_{(\alpha'\beta'\gamma'|\alpha\beta\gamma)}^{(i'j'k'|ijk)}(p)$ defined in (2.2).

One aspect of the FORCER package is that it only evaluates Feynman integrals which are Lorentz invariants. Therefore loop momenta embedded in γ matrix strings have to be accommodated first.

As in [13] this is carried out using what is now a standard projection procedure. It is straightforward to withdraw the loop momenta from the γ matrices to leave a tensor integral for each graph where the rank is an even integer. For instance for a four loop graph in the Feynman gauge the highest rank of an integral is eight. As each tensor integral has even rank it will be equal to a sum of rank eight tensors built from the metric $\eta_{\mu\nu}$ and the sole external momentum p_μ . There are 764 independent tensors that the rank eight integral decomposes into and mapping the integral to this basis is achieved by constructing and inverting a 764×764 matrix. Clearly this is a huge exercise. However as the integral rank is even and there is only one independent external momentum one can ensure that the matrix is sparse by redefining the tensors of the decomposition into transverse, $P_{\mu\nu}(p)$, and longitudinal $L_{\mu\nu}(p)$ projectors instead of combinations of $\eta_{\mu\nu}$ and p_μ where

$$P_{\mu\nu}(p) = \eta_{\mu\nu} - \frac{p_\mu p_\nu}{p^2} \quad , \quad L_{\mu\nu}(p) = \frac{p_\mu p_\nu}{p^2} \quad . \quad (2.7)$$

The benefit of this choice rests in the algebra of the projectors which is

$$P_\mu^\sigma(p)P_{\sigma\nu}(p) = P_{\mu\nu}(p) \quad , \quad L_\mu^\sigma(p)L_{\sigma\nu}(p) = L_{\mu\nu}(p) \quad , \quad P_\mu^\sigma(p)L_{\sigma\nu}(p) = 0 \quad (2.8)$$

and has the useful property that the matrix is block diagonal. Using this approach we have constructed the four general projection tensors up to rank eight to carry out the four loop renormalization of the baryon operator in the Feynman gauge. As a check on this routine we have reproduced the two and three loop results of [12, 13] for an arbitrary gauge parameter as originally that renormalization was carried out in the Feynman gauge. Therefore all the tensor integrals can be written in terms of numerator scalar products and $P_{\mu\nu}(p)$ and $L_{\mu\nu}(p)$. The contraction of the Lorentz indices of these two projectors with the original γ strings produces strings involving contracted Lorentz indices or the external momenta.

While the resulting scalar integrals involve scalar products of the external and loop momenta, which could in principle be passed to the FORCER algorithm in our automated Feynman integral evaluation code, there is a large amount of associated accompanying γ algebra which would slow the actual integration. As the computation is dimensionally regularized the Clifford algebra of the four dimensional γ algebra is no longer finite dimensional but instead is infinite dimensional. Therefore the three open γ strings need to be mapped to the basis of d -dimensional γ matrices in the same way as the two and three loop computations of [12, 13] were. This basis was introduced and discussed in [27, 28, 29, 30, 31] and consists of the countably infinite set of matrices $\Gamma_{(n)}^{\mu_1 \dots \mu_n}$ where the integer n lies in the range $0 \leq n < \infty$. These generalized γ matrices are totally antisymmetric in the Lorentz indices and defined by

$$\Gamma_{(n)}^{\mu_1 \dots \mu_n} = \gamma^{[\mu_1} \dots \gamma^{\mu_n]} \quad (2.9)$$

where a factor of $1/n!$ is understood. The finer details of the algebra that they satisfy is discussed in [30, 31]. It is important to remember that the basis is infinite when the spacetime dimension d is not an integer. If d is an integer the basis reduces substantially to a finite set. For instance in four dimensions it corresponds to

$$\begin{aligned} \Gamma_{(0)} \Big|_{d=4} &= \mathcal{I} \quad , \quad \Gamma_{(1)}^\mu \Big|_{d=4} = \gamma^\mu \quad , \quad \Gamma_{(2)}^{\mu\nu} \Big|_{d=4} = \sigma^{\mu\nu} \\ \Gamma_{(3)}^{\mu\nu\sigma} \Big|_{d=4} &= \epsilon^{\mu\nu\sigma\rho} \gamma^5 \gamma_\rho \quad , \quad \Gamma_{(4)}^{\mu\nu\sigma\rho} \Big|_{d=4} = \epsilon^{\mu\nu\sigma\rho} \gamma^5 \quad , \quad \Gamma_{(n)}^{\mu_1 \dots \mu_n} \Big|_{d=4} = 0 \quad \text{for } n \geq 5 \end{aligned} \quad (2.10)$$

where \mathcal{I} is the unit matrix in four dimensions, $\Gamma_{(0)}$ is regarded as the d -dimensional unit matrix and $\sigma^{\mu\nu} = \frac{1}{2}[\gamma^\mu, \gamma^\nu]$. The collapse to five non-trivial matrices in this dimension means that in $d = 4 - 2\epsilon$ dimensions, when ϵ is small, one can regard any operator involving $\Gamma_{(n)}^{\mu_1 \dots \mu_n}$ for $n \geq 5$ as evanescent. In other words while they are absent in the critical dimension of the theory their

presence in the regularized theory cannot be neglected in the limit to four dimensions when the regularization is lifted. This is not unconnected with the definition of γ^5 which is a purely four dimension matrix with no natural analytic continuation to the dimensionally regularized theory. However we note that γ^5 has no connection whatsoever with $\Gamma_{(5)}^{\mu_1 \dots \mu_5}$. In [32] a procedure was developed that allowed for the renormalization of γ^5 dependent quark bilinear operators to high loop order using the $\Gamma_{(n)}$ matrices. Briefly this involved the introduction of a finite renormalization that restored and ensured the chiral symmetry property of the operators in four dimensions was respected. The generalized γ matrices that we employ here have several useful properties such as, [29, 30, 31],

$$\Gamma_{(n)}^{\mu_1 \dots \mu_n} \gamma^\nu = \Gamma_{(n+1)}^{\mu_1 \dots \mu_n \nu} + \sum_{r=1}^n (-1)^{n-r} \eta^{\mu_r \nu} \Gamma_{(n-1)}^{\mu_1 \dots \mu_{r-1} \mu_{r+1} \dots \mu_n} \quad (2.11)$$

$$\gamma^\nu \Gamma_{(n)}^{\mu_1 \dots \mu_n} = \Gamma_{(n+1)}^{\nu \mu_1 \dots \mu_n} + \sum_{r=1}^n (-1)^{r-1} \eta^{\mu_r \nu} \Gamma_{(n-1)}^{\mu_1 \dots \mu_{r-1} \mu_{r+1} \dots \mu_n} \quad (2.12)$$

which allows us to recursively map the three γ strings of $G_{(\alpha' \beta' \gamma' | \alpha \beta \gamma)}$ to the $\Gamma_{(n)}$ basis. In particular the three γ strings can be written in terms of the objects

$$\Gamma_{qrs(\alpha \alpha' | \beta \beta' | \gamma \gamma')} = \Gamma_{(q)\alpha \alpha'} \otimes \Gamma_{(r)\beta \beta'} \otimes \Gamma_{(s)\gamma \gamma'} \quad (2.13)$$

where q , r and s will be even from the fact that this is a massless computation. The spinor indices are included for reference when it comes to their multiplication for instance but will omitted hereafter.

In indicating this spinor structure the Lorentz indices have been suppressed as it is not possible to easily accommodate them in a general way. The explicit Lorentz contracted versions that actually arise to four loops will be provided later. Not only will there be contractions of indices across strings but the Γ_{qrs} can contain at most two external momenta with each on a separate string due to the antisymmetry of the $\Gamma_{(n)}$ matrices. Such external momenta dependent Γ_{qrs} matrices cannot be present in the final renormalization constant for $\mathcal{O}_{\alpha \beta \gamma}^{ijk}$ since the operator associated with them would invalidate renormalizability. They can be and are present in the evaluation of an individual graph but have to cancel upon summation of all the graphs. As an orientation point we have provided an example of a graph which contains Γ_{484} in Figure 2 where the labelling is from the left in the graph. The convention is that the subscripts count the number of γ matrices in each quark line starting from the left. There will be other Γ_{qrs} matrices in this graph due to contractions but with lower subscript values.

While the Γ_{qrs} matrices form the core structure of the γ strings of a graph a more general combination emerges in the renormalization constant of \mathcal{O}^{ijk} . These are denoted by \mathbb{C}_{qrs} and are symmetric in the even integers q , r and s . In particular there are three classes of \mathbb{C}_{qrs} given explicitly by

$$\begin{aligned} \mathbb{C}_{qqq} &\equiv \Gamma_{qqq} \quad , \quad \mathbb{C}_{qqr} \equiv \Gamma_{qqr} + \Gamma_{qrq} + \Gamma_{rqq} = \mathbb{C}_{qrq} = \mathbb{C}_{rqq} \\ \mathbb{C}_{qrs} &\equiv \Gamma_{qrs} + \Gamma_{qsr} + \Gamma_{rqs} + \Gamma_{rsq} + \Gamma_{srq} + \Gamma_{sqr} \end{aligned} \quad (2.14)$$

where there is no summation over repeated labels, q , r and s are all different here and we will use the convention that the integers in the explicit label of a particular \mathbb{C}_{qrs} will be in descending order. To four loops the objects that are present in the renormalization constant are

$$\begin{aligned} \mathbb{C}_{000} &= \Gamma_{000} \quad , \quad \mathbb{C}_{220} = \Gamma_{220} + \Gamma_{202} + \Gamma_{022} \\ \mathbb{C}_{440} &= \Gamma_{440} + \Gamma_{404} + \Gamma_{044} \quad , \quad \mathbb{C}_{422} = \Gamma_{422} + \Gamma_{242} + \Gamma_{224} \\ \mathbb{C}_{660} &= \Gamma_{660} + \Gamma_{606} + \Gamma_{066} \quad , \quad \mathbb{C}_{444} = \Gamma_{444} \end{aligned}$$

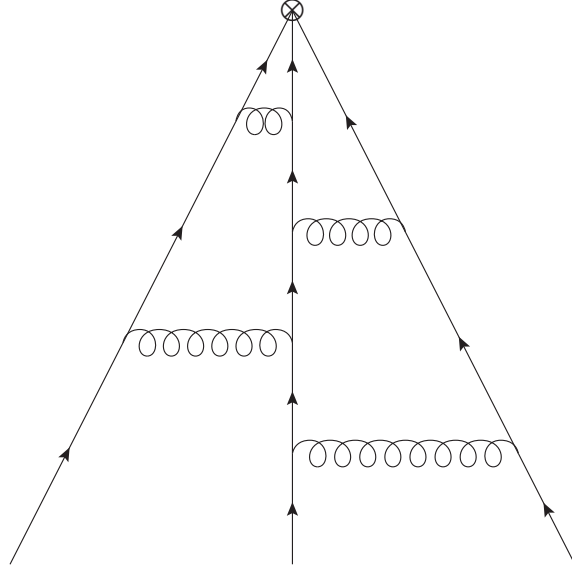


Figure 2: Four loop graph contribution to $G_{(\alpha'\beta'\gamma'|\alpha\beta\gamma)}^{(i'j'k'|ijk)}(p)$ containing the γ matrix structure Γ_{484} .

$$\begin{aligned}
\mathbb{C}_{642} &= \Gamma_{642} + \Gamma_{624} + \Gamma_{462} + \Gamma_{426} + \Gamma_{246} + \Gamma_{264} \\
\mathbb{C}_{880} &= \Gamma_{880} + \Gamma_{808} + \Gamma_{088} \\
\mathbb{C}_{862} &= \Gamma_{862} + \Gamma_{826} + \Gamma_{682} + \Gamma_{628} + \Gamma_{268} + \Gamma_{286} \\
\mathbb{C}_{844} &= \Gamma_{844} + \Gamma_{484} + \Gamma_{448} \quad , \quad \mathbb{C}_{664} = \Gamma_{664} + \Gamma_{646} + \Gamma_{466} \quad .
\end{aligned} \tag{2.15}$$

However at intermediate steps

$$\begin{aligned}
\mathbb{C}_{222} &= \Gamma_{222} \quad , \quad \mathbb{C}_{442} = \Gamma_{442} + \Gamma_{424} + \Gamma_{244} \\
\mathbb{C}_{662} &= \Gamma_{662} + \Gamma_{626} + \Gamma_{266} \quad , \quad \mathbb{C}_{644} = \Gamma_{644} + \Gamma_{464} + \Gamma_{446}
\end{aligned} \tag{2.16}$$

will also arise but when all the graphs are summed they are absent. We note that for each of these the sum of the q , r and s labels is not a multiple of four. Within each \mathbb{C}_{qrs} definition the Lorentz index contractions are

$$\begin{aligned}
\Gamma_{000} &= \Gamma_{(0)} \otimes \Gamma_{(0)} \otimes \Gamma_{(0)} \\
\Gamma_{220} &= \Gamma_{(2)}^{\mu_1\mu_2} \otimes \Gamma_{(2)\mu_1\mu_2} \otimes \Gamma_{(0)} \\
\Gamma_{440} &= \Gamma_{(4)}^{\mu_1\mu_2\mu_3\mu_4} \otimes \Gamma_{(4)\mu_1\mu_2\mu_3\mu_4} \otimes \Gamma_{(0)} \\
\Gamma_{422} &= \Gamma_{(4)}^{\mu_1\mu_2\mu_3\mu_4} \otimes \Gamma_{(2)\mu_1\mu_2} \otimes \Gamma_{(2)\mu_3\mu_4} \\
\Gamma_{660} &= \Gamma_{(6)}^{\mu_1\mu_2\mu_3\mu_4\mu_5\mu_6} \otimes \Gamma_{(6)\mu_1\mu_2\mu_3\mu_4\mu_5\mu_6} \otimes \Gamma_{(0)} \\
\Gamma_{444} &= \Gamma_{(4)}^{\mu_1\mu_2\mu_3\mu_4} \otimes \Gamma_{(4)\mu_1\mu_2}^{\mu_5\mu_6} \otimes \Gamma_{(4)\mu_3\mu_4\mu_5\mu_6} \\
\Gamma_{642} &= \Gamma_{(6)}^{\mu_1\mu_2\mu_3\mu_4\mu_5\mu_6} \otimes \Gamma_{(4)\mu_1\mu_2\mu_3\mu_4} \otimes \Gamma_{(2)\mu_5\mu_6} \\
\Gamma_{880} &= \Gamma_{(8)}^{\mu_1\mu_2\mu_3\mu_4\mu_5\mu_6\mu_7\mu_8} \otimes \Gamma_{(8)\mu_1\mu_2\mu_3\mu_4\mu_5\mu_6\mu_7\mu_8} \otimes \Gamma_{(0)} \\
\Gamma_{862} &= \Gamma_{(8)}^{\mu_1\mu_2\mu_3\mu_4\mu_5\mu_6\mu_7\mu_8} \otimes \Gamma_{(6)\mu_1\mu_2\mu_3\mu_4\mu_5\mu_6} \otimes \Gamma_{(2)\mu_7\mu_8} \\
\Gamma_{844} &= \Gamma_{(8)}^{\mu_1\mu_2\mu_3\mu_4\mu_5\mu_6\mu_7\mu_8} \otimes \Gamma_{(4)\mu_1\mu_2\mu_3\mu_4} \otimes \Gamma_{(4)\mu_5\mu_6\mu_7\mu_8} \\
\Gamma_{664} &= \Gamma_{(6)}^{\mu_1\mu_2\mu_3\mu_4\mu_5\mu_6} \otimes \Gamma_{(6)\mu_1\mu_2\mu_3\mu_4\mu_7\mu_8} \otimes \Gamma_{(4)\mu_5\mu_6}^{\mu_7\mu_8}
\end{aligned} \tag{2.17}$$

for those γ strings that arise in the renormalization appearing for the first time at L loops where

$q + r + s = 4L$. For the remainder

$$\begin{aligned}
\Gamma_{222} &= \Gamma_{(2)}^{\mu_1\mu_2} \otimes \Gamma_{(2)}^{\mu_1\mu_3} \otimes \Gamma_{(2)}^{\mu_2\mu_3} \\
\Gamma_{442} &= \Gamma_{(4)}^{\mu_1\mu_2\mu_3\mu_4} \otimes \Gamma_{(4)}^{\mu_1\mu_2\mu_3} \otimes \Gamma_{(2)}^{\mu_4\mu_5} \\
\Gamma_{662} &= \Gamma_{(6)}^{\mu_1\mu_2\mu_3\mu_4\mu_5\mu_6} \otimes \Gamma_{(6)}^{\mu_1\mu_2\mu_3\mu_4\mu_5\mu_7} \otimes \Gamma_{(2)}^{\mu_6\mu_7} \\
\Gamma_{644} &= \Gamma_{(6)}^{\mu_1\mu_2\mu_3\mu_4\mu_5\mu_6} \otimes \Gamma_{(4)}^{\mu_1\mu_2\mu_3\mu_7} \otimes \Gamma_{(4)}^{\mu_4\mu_5\mu_6\mu_7}
\end{aligned} \tag{2.18}$$

where the contractions for the permuted distinct q , r and s labels are deduced in an obvious fashion. In addition there are γ strings which involve contractions with the external momenta p such as

$$\begin{aligned}
\Gamma_{2p2p2} &= \Gamma_{(2)}^{p\mu_1} \otimes \Gamma_{(2)}^{p\mu_2} \otimes \Gamma_{(2)}^{\mu_1\mu_2} \\
\Gamma_{22p4p} &= \Gamma_{(2)}^{\mu_1\mu_2} \otimes \Gamma_{(2)}^{p\mu_3} \otimes \Gamma_{(4)}^{p\mu_1\mu_2\mu_3} \\
\Gamma_{24p4p} &= \Gamma_{(2)}^{\mu_1\mu_2} \otimes \Gamma_{(4)}^{p\mu_1\mu_3\mu_4} \otimes \Gamma_{(4)}^{p\mu_2\mu_3\mu_4} \\
\Gamma_{2p4p4} &= \Gamma_{(2)}^{p\mu_1} \otimes \Gamma_{(4)}^{p\mu_2\mu_3\mu_4} \otimes \Gamma_{(4)}^{\mu_1\mu_2\mu_3\mu_4} \\
\Gamma_{4p4p4} &= \Gamma_{(4)}^{p\mu_1\mu_2\mu_5} \otimes \Gamma_{(4)}^{p\mu_3\mu_4} \otimes \Gamma_{(4)}^{\mu_1\mu_2\mu_3\mu_4} \\
\Gamma_{24p6p} &= \Gamma_{(2)}^{\mu_1\mu_2} \otimes \Gamma_{(4)}^{p\mu_3\mu_4\mu_5} \otimes \Gamma_{(6)}^{p\mu_1\mu_2\mu_3\mu_4\mu_5} \\
\Gamma_{26p6p} &= \Gamma_{(2)}^{\mu_1\mu_2} \otimes \Gamma_{(6)}^{p\mu_1\mu_3\mu_4\mu_5\mu_6} \otimes \Gamma_{(6)}^{p\mu_2\mu_3\mu_4\mu_5\mu_6} \\
\Gamma_{4p4p6} &= \Gamma_{(4)}^{p\mu_1\mu_2\mu_3} \otimes \Gamma_{(4)}^{p\mu_4\mu_5\mu_6} \otimes \Gamma_{(6)}^{\mu_1\mu_2\mu_3\mu_4\mu_5\mu_6} \\
\Gamma_{46p6p} &= \Gamma_{(4)}^{\mu_1\mu_2\mu_3\mu_4} \otimes \Gamma_{(6)}^{p\mu_1\mu_2\mu_5\mu_6\mu_7} \otimes \Gamma_{(6)}^{p\mu_3\mu_4\mu_5\mu_6\mu_7} \\
\Gamma_{nnpn0} &= \Gamma_{(n)}^{p\mu_1\dots\mu_{n-1}} \otimes \Gamma_{(n)}^{p\mu_1\dots\mu_{n-1}} \otimes \Gamma_{(0)}
\end{aligned} \tag{2.19}$$

where n is even and we use the convention that the appearance of p in the index string corresponds to its contraction with a Lorentz index. In the overall determination of the operator renormalization constants the poles in ϵ associated with these structures cancel. Otherwise the original operator would be non-renormalizable as they would have to have a factor of $1/p^2$ on dimensional grounds and therefore would correspond to a non-local 3-quark operator.

Having introduced the compact notation for the underlying γ matrix structure that is associated with (2.2) we can now introduce the renormalization constant for \mathcal{O}^{ijk} . Denoting bare quantities with the subscript o then

$$\mathcal{O}_{o\alpha\beta\gamma}^{ijk} = Z_{\alpha\beta\gamma}^{\alpha'\beta'\gamma'} \mathcal{O}_{\alpha'\beta'\gamma'}^{ijk} . \tag{2.20}$$

Explicit computations indicate the renormalization constant takes the form

$$Z_{\alpha\alpha'\beta\beta'\gamma\gamma'} = \mathbb{C}_{000(\alpha\alpha'|\beta\beta'|\gamma\gamma')} + \sum_{\mathcal{K}} a_{qrs}(\epsilon) \mathbb{C}_{qrs(\alpha\alpha'|\beta\beta'|\gamma\gamma')} \tag{2.21}$$

where the indexing set \mathcal{K} ranges over all valid combinations of q , r and s of the basic $\Gamma_{(n)}$ matrix structure and thus there is no sum over individual q , r and s . The ϵ dependent poles are contained in

$$a_{qrs}(\epsilon) = \sum_{n=1}^{\infty} \frac{a_{qrs}^{(n)}}{\epsilon^n} \tag{2.22}$$

where we have chosen to renormalize in the $\overline{\text{MS}}$ scheme. To extract the particular residues we have evaluated all the Feynman graphs to four loops contributing to (2.2) for the momentum configuration of Figure 1. As this is in effect a 2-point function the FORCER algorithm of [15, 16] can be applied. The Feynman graphs are generated with QGRAF [33] and there are 3, 40, 784 and 19061 graphs from one to four loops respectively. A central aspect of the evaluation is the mapping of the γ matrix structures that arise to the \mathbb{C}_{qrs} basis in a way that is algebraically manageable for which FORM was the ideal tool.

3 Results.

Having described the basic structures of the renormalization process for (2.2) we have extracted the four loop renormalization constant for $\mathcal{O}_{\alpha\beta\gamma}^{ijk}$ in terms of the general \mathbb{C}_{qrs} basis in the $\overline{\text{MS}}$ scheme. Its conversion to the associated operator anomalous dimension is effected via the spinor equation

$$\gamma_{\mathcal{O}\alpha\alpha''\beta\beta''\gamma\gamma''}(a)Z_{\mathcal{O}}^{\alpha''\beta''\gamma''}_{\alpha'\beta'\gamma'} = Z_{\mathcal{O}\alpha\alpha''\beta\beta''\gamma\gamma''}\gamma_{\mathcal{O}}^{\alpha''\beta''\gamma''}_{\alpha'\beta'\gamma'}(a) = \beta(a)\frac{\partial}{\partial a}Z_{\mathcal{O}\alpha\alpha'\beta\beta'\gamma\gamma'} \quad (3.1)$$

which is the functional generalization of the usual derivative of the logarithm of a renormalization constant and where a is the coupling constant. The operator anomalous dimension has to be defined in this manner since the logarithm of a matrix only has meaning in a perturbative or Taylor series sense. The equivalence of (3.1) to the canonical definition of an anomalous dimension is preserved by the separate left and right multiplications. Both have to lead to the same value of $\gamma_{\mathcal{O}}(a)$. The final stage of extracting the anomalous dimension involves the multiplications on the left side of (3.1) which involve products of \mathbb{C}_{qrs} . We have provided the relations that were needed to four loops in Appendix A. As the labels of \mathbb{C}_{qrs} that contribute to the anomalous dimension sum to multiples of $4n$ for positive integers n the sum of the labels of the product of two \mathbb{C}_{qrs} needed for a four loop renormalization must be no more than 16 which is 4 times the loop order. Therefore there are 1, 2 and 6 relevant products at two, three and four loops respectively excluding those involving the identity \mathbb{C}_{000} . Consequently we find the anomalous dimension is

$$\begin{aligned} \gamma_{\mathcal{O}}^{\text{naive}}(a) = & \left[\frac{1}{3}a + \left[\frac{49}{18} - \frac{1}{27}N_f \right] a^2 + \left[\frac{5479}{108} - \frac{212}{81}N_f - \frac{127}{9}\zeta_3 - \frac{40}{9}\zeta_3N_f - \frac{13}{81}N_f^2 \right] a^3 \right. \\ & + \left[\frac{16}{81}\zeta_3N_f^3 + \frac{440}{81}\zeta_3N_f^2 + \frac{533}{9}\zeta_4N_f + \frac{1397}{6}\zeta_4 + \frac{1705}{1458}N_f^2 + \frac{5380}{27}\zeta_5N_f \right. \\ & + \left. \frac{2320925}{1944} - \frac{300335}{486}\zeta_5 - \frac{266069}{972}\zeta_3 - \frac{150629}{972}N_f - \frac{39731}{162}\zeta_3N_f - \frac{40}{9}\zeta_4N_f^2 \right. \\ & \left. \left. - \frac{5}{27}N_f^3 \right] a^4 \right] \mathbb{C}_{220} \\ & + \left[[4N_f - 70] a^2 + \left[\frac{434}{3}\zeta_3 + \frac{1708}{9}N_f - \frac{16492}{9} - \frac{20}{9}N_f^2 \right] a^3 \right. \\ & + \left[\frac{434}{3}\zeta_4N_f + \frac{5555}{27}\zeta_5 + \frac{14900}{27}\zeta_3N_f + \frac{172582}{27}N_f + \frac{212572}{27}\zeta_3 - 2387\zeta_4 \right. \\ & \left. \left. - 280\zeta_5N_f - \frac{374575}{9} - \frac{1285}{9}N_f^2 - \frac{160}{3}\zeta_3N_f^2 - \frac{140}{81}N_f^3 \right] a^4 \right] \mathbb{C}_{000} \\ & + \left[-\frac{1}{9}a^2 + \left[\frac{2}{81}N_f + \frac{13}{36}\zeta_3 + \frac{127}{216} \right] a^3 \right. \\ & + \left[\frac{13}{36}\zeta_4N_f + \frac{299}{2916}N_f^2 + \frac{829}{324}\zeta_3N_f + \frac{3287}{1944}N_f + \frac{97705}{1944}\zeta_5 - \frac{45415}{1944}\zeta_3 \right. \\ & \left. \left. - \frac{13045}{324} - \frac{143}{24}\zeta_4 - \frac{5}{3}\zeta_5N_f \right] a^4 \right] \mathbb{C}_{440} \\ & + \left[\frac{1}{18}a^2 + \left[\frac{1}{162}N_f + \frac{19}{27} + \frac{25}{18}\zeta_3 \right] a^3 \right. \\ & + \left[\frac{25}{18}\zeta_4N_f + \frac{695}{72} + \frac{5549}{243}\zeta_3 - \frac{15545}{972}\zeta_5 - \frac{1127}{972}N_f - \frac{275}{12}\zeta_4 - \frac{77}{81}\zeta_3N_f \right. \\ & \left. \left. - \frac{40}{9}\zeta_5N_f - \frac{37}{729}N_f^2 \right] a^4 \right] \mathbb{C}_{422} \\ & + \left[\left[\frac{59}{432}\zeta_3 - \frac{101}{1296} \right] a^3 \right. \end{aligned}$$

$$\begin{aligned}
& + \left[\frac{59}{432} \zeta_4 N_f + \frac{10535}{7776} + \frac{21293}{1944} \zeta_3 - \frac{128585}{7776} \zeta_5 - \frac{649}{288} \zeta_4 - \frac{389}{11664} N_f \right. \\
& \quad \left. - \frac{295}{3888} \zeta_3 N_f \right] a^4 \mathbb{C}_{660} \\
& + \left[-\frac{17}{216} a^3 + \left[\frac{23}{162} \zeta_3 N_f + \frac{1087}{1296} \zeta_3 - \frac{6775}{1296} \zeta_5 - \frac{6727}{1296} - \frac{257}{1944} N_f \right] a^4 \right] \mathbb{C}_{444} \\
& + \left[\left[\frac{1}{16} \zeta_3 - \frac{1}{16} \right] a^3 \right. \\
& \quad \left. + \left[\frac{1}{16} \zeta_4 N_f + \frac{9037}{7776} + \frac{9295}{648} \zeta_3 - \frac{47675}{2592} \zeta_5 - \frac{125}{3888} N_f - \frac{33}{32} \zeta_4 - \frac{5}{144} \zeta_3 N_f \right] a^4 \right] \mathbb{C}_{642} \\
& + \left[\left[\frac{25}{972} \zeta_5 + \frac{31}{15552} - \frac{1411}{15552} \zeta_3 \right] \mathbb{C}_{880} + \left[\frac{205}{1944} \zeta_5 - \frac{247}{7776} \zeta_3 - \frac{113}{1944} \right] \mathbb{C}_{862} \right. \\
& \quad \left. + \left[\frac{149}{2592} \zeta_3 - \frac{35}{3888} - \frac{5}{48} \zeta_5 \right] \mathbb{C}_{844} + \left[\frac{55}{216} \zeta_5 - \frac{61}{864} \zeta_3 - \frac{29}{216} \right] \mathbb{C}_{664} \right] a^4 \\
& + O(a^5) . \tag{3.2}
\end{aligned}$$

where ζ_n is the Riemann zeta function. In terms of conventions for this anomalous dimension we follow those of [20] where the one loop term has a factor of $\frac{1}{3}$ in contrast to the convention used in [13]. It is evident that no \mathbb{C}_{qrs} appears before loop order L where $L = \frac{1}{4}(q+r+s)$ here which acts as an accounting check. Numerically (3.2) is

$$\begin{aligned}
\gamma_{\mathcal{O}}^{\text{naive}}(a) & = 0.333333\mathbb{C}_{220}a \\
& + [[4.000000N_f - 70.000000] \mathbb{C}_{000} + [2.722222 - 0.037037N_f] \mathbb{C}_{220} + 0.055556\mathbb{C}_{422} \\
& \quad - 0.111111\mathbb{C}_{440}] a^2 \\
& + [[189.777778N_f - 2.222222N_f^2 - 1658.546879] \mathbb{C}_{000} \\
& \quad + [33.769123 - 0.160494N_f^2 - 7.959759N_f] \mathbb{C}_{220} \\
& \quad + [0.006173N_f + 2.373227] \mathbb{C}_{422} + [0.024691N_f + 1.022039] \mathbb{C}_{440} + 0.012629\mathbb{C}_{642} \\
& \quad + 0.086238\mathbb{C}_{660} - 0.078704\mathbb{C}_{444}] a^3 \\
& + [[6921.519577N_f - 1.728395N_f^3 - 206.887479N_f^2 - 34525.773200] \mathbb{C}_{000} \\
& \quad + [0.052258N_f^3 + 2.888776N_f^2 - 179.061229N_f + 476.055481] \mathbb{C}_{220} \\
& \quad + [-0.050754N_f^2 - 5.407502N_f - 4.284400] \mathbb{C}_{422} + 0.044906\mathbb{C}_{664} \\
& \quad + [0.102538N_f^2 + 3.429103N_f - 22.677437] \mathbb{C}_{440} + [0.038461N_f - 9.603048] \mathbb{C}_{444} \\
& \quad + [-0.006243N_f - 1.783863] \mathbb{C}_{642} + [0.023261N_f - 5.064598] \mathbb{C}_{660} \\
& \quad - 0.047916\mathbb{C}_{844} + 0.013037\mathbb{C}_{862} - 0.080397\mathbb{C}_{880}] a^4 + O(a^5) . \tag{3.3}
\end{aligned}$$

We have given the label naive to the anomalous dimension of (3.2) for a particular reason. It is the anomalous dimension of \mathcal{O} in the regularized theory with $\epsilon \neq 0$. Ordinarily the passage back to four dimensions is straightforward in the limit of $\epsilon \rightarrow 0$. However this limit cannot be taken immediately since (3.2) contains evanescent \mathbb{C}_{qrs} structures which correspond to any one of of q , r or s being strictly more than 4 as is apparent from (2.10). To extract an anomalous dimension for \mathcal{O} in four dimensions requires an additional procedure which was introduced in [13] and motivated by a relation used in the two loop computation of [12]. The basic idea at two loops was to realize that not all the \mathbb{C}_{qrs} which appear are independent since, for instance,

$$\mathbb{C}_{422} = -3d(d-1)\mathbb{C}_{000} - 2(d-3)\mathbb{C}_{220} - \frac{1}{2}\mathbb{C}_{440} + \frac{1}{2}\mathbb{C}_{220}^2 \tag{3.4}$$

was derived in [12]. While \mathbb{C}_{422} is not related to an evanescent structure it was expressed in terms of the other \mathbb{C}_{qrs} since the eigenvalues of \mathbb{C}_{220} and \mathbb{C}_{440} could be determined for four dimensional baryon operators [12] which we will recall later. However similar d -dimensional relations can be established for evanescent \mathbb{C}_{qrs} structures and three loop ones were given in [13] which were

$$\begin{aligned}
\mathbb{C}_{660} &= -12d(d-1)(2d-1)\mathbb{C}_{000} - 3(d-1)(7d-24)\mathbb{C}_{220} - 6(2d-5)\mathbb{C}_{440} \\
&\quad + 2(3d-4)\mathbb{C}_{220}^2 - \frac{1}{2}\mathbb{C}_{220}^3 + \frac{3}{2}\mathbb{C}_{220}\mathbb{C}_{440} + 3\mathbb{C}_{444} \\
\mathbb{C}_{642} &= 12d(d-1)(2d-7)\mathbb{C}_{000} + 9(d^2-9d+16)\mathbb{C}_{220} + 2(2d-5)\mathbb{C}_{440} \\
&\quad - 2(3d-10)\mathbb{C}_{220}^2 + \frac{1}{2}\mathbb{C}_{220}^3 - \frac{1}{2}\mathbb{C}_{220}\mathbb{C}_{440} - 3\mathbb{C}_{444} .
\end{aligned} \tag{3.5}$$

The procedure to establish these relations is clear. The two loop relation of (3.4) involves the square of the one loop structure which is \mathbb{C}_{220} . In fact evaluating the square was the starting point to deduce (3.4). At three loops to produce the evanescent structures there are two possible combinations of \mathbb{C}_{220} and \mathbb{C}_{440} that will lead to the two three loop evanescent \mathbb{C}_{qrs} structures. These are \mathbb{C}_{220}^3 and $\mathbb{C}_{220}\mathbb{C}_{440}$ which both have a total $(q+r+s)$ value of 12. Evaluating these lead to the relations of (3.5).

Therefore the algorithm is set to construct the relations for the four loop evanescent \mathbb{C}_{qrs} structures. Since there are four such objects then we require four combinations of lower order non-evanescent \mathbb{C}_{qrs} objects. Clearly the starting point for these are \mathbb{C}_{220}^4 , $\mathbb{C}_{220}^2\mathbb{C}_{440}$, \mathbb{C}_{440}^2 and $\mathbb{C}_{220}\mathbb{C}_{444}$ as \mathbb{C}_{444} is non-evanescent and appears first at three loops. Evaluating these products produces four linear combinations of \mathbb{C}_{880} , \mathbb{C}_{862} , \mathbb{C}_{844} and \mathbb{C}_{664} and inverting them gives

$$\begin{aligned}
\mathbb{C}_{880} &= 6d(d-1)(69d^2-437d+280)\mathbb{C}_{000} - \frac{1}{2}\mathbb{C}_{220}^4 + 16(d-4)\mathbb{C}_{220}^3 + \mathbb{C}_{220}^2\mathbb{C}_{440} \\
&\quad - 2(65d^2-437d+512)\mathbb{C}_{220}^2 - 8(4d-19)\mathbb{C}_{220}\mathbb{C}_{440} + 4\mathbb{C}_{220}\mathbb{C}_{444} - 24(3d-22)\mathbb{C}_{444} \\
&\quad + 16(16d^3-183d^2+545d-384)\mathbb{C}_{220} + \frac{1}{2}\mathbb{C}_{440}^2 + 6(23d^2-175d+256)\mathbb{C}_{440} \\
\mathbb{C}_{862} &= -6d(d-1)(21d^2-245d+556)\mathbb{C}_{000} - (4d-35)\mathbb{C}_{220}^2 + \frac{1}{2}\mathbb{C}_{220}^2\mathbb{C}_{440} + 6(6d-67)\mathbb{C}_{444} \\
&\quad + (37d^2-433d+976)\mathbb{C}_{220}^2 + (2d-29)\mathbb{C}_{220}\mathbb{C}_{440} - \mathbb{C}_{220}\mathbb{C}_{444} \\
&\quad - 2(14d^3-303d^2+1801d-2640)\mathbb{C}_{220} - \frac{1}{2}\mathbb{C}_{440}^2 - 12(2d^2-18d+23)\mathbb{C}_{440} \\
\mathbb{C}_{844} &= -3d(d-1)(17d^2-81d+160)\mathbb{C}_{000} + \frac{1}{4}\mathbb{C}_{220}^4 - 4(d-2)\mathbb{C}_{220}^3 - \frac{1}{2}\mathbb{C}_{220}^2\mathbb{C}_{440} \\
&\quad + (17d^2-85d+128)\mathbb{C}_{220}^2 + 4(d-1)\mathbb{C}_{220}\mathbb{C}_{440} - 2\mathbb{C}_{220}\mathbb{C}_{444} + 12(d+8)\mathbb{C}_{444} \\
&\quad - 8(d^3-18d^2+71d-96)\mathbb{C}_{220} + \frac{1}{4}\mathbb{C}_{440}^2 - 3(3d^2-11d+24)\mathbb{C}_{440} \\
\mathbb{C}_{664} &= 6d(d-1)(d^2-d-8)\mathbb{C}_{000} + \mathbb{C}_{220}^3 - (d^2+3d-20)\mathbb{C}_{220}^2 - \mathbb{C}_{220}\mathbb{C}_{440} + \mathbb{C}_{220}\mathbb{C}_{444} \\
&\quad - 6(2d-7)\mathbb{C}_{444} + 2(2d^3-15d^2+13d+24)\mathbb{C}_{220} + d(d-1)\mathbb{C}_{440}
\end{aligned} \tag{3.6}$$

in d -dimensions. The right hand side of each of these and the lower order ones contain only \mathbb{C}_{qrs} structures with individual q , r or s values of 0, 2 or 4. It is these relations that will allow us to construct an anomalous dimension for \mathcal{O} in four dimensions.

However it is worth recording the argument for the five and six loop cases in order to appreciate the subtlety of the above derivation. At five loops there are five evanescent objects and precisely five independent combinations of \mathbb{C}_{220} , \mathbb{C}_{440} and \mathbb{C}_{444} with 10 contracted Lorentz indices. The five relations can be constructed from the basis mapping

$$\{\mathbb{C}_{10100}, \mathbb{C}_{1082}, \mathbb{C}_{1064}, \mathbb{C}_{884}, \mathbb{C}_{866}\} \leftrightarrow \{\mathbb{C}_{220}^5, \mathbb{C}_{220}^3\mathbb{C}_{440}, \mathbb{C}_{220}\mathbb{C}_{440}^2, \mathbb{C}_{220}^2\mathbb{C}_{444}, \mathbb{C}_{440}\mathbb{C}_{444}\} . \tag{3.7}$$

At six loops the number of evanescent structures and independent combinations is seven. Specifically

$$\begin{aligned} & \{\mathbb{C}_{12120}, \mathbb{C}_{12102}, \mathbb{C}_{1284}, \mathbb{C}_{1266}, \mathbb{C}_{10104}, \mathbb{C}_{1086}, \mathbb{C}_{888}\} \\ & \leftrightarrow \{\mathbb{C}_{220}^6, \mathbb{C}_{220}^4 \mathbb{C}_{440}, \mathbb{C}_{220}^2 \mathbb{C}_{440}^2, \mathbb{C}_{440}^3, \mathbb{C}_{220}^3 \mathbb{C}_{444}, \mathbb{C}_{220} \mathbb{C}_{440} \mathbb{C}_{444}, \mathbb{C}_{444}^2\} \end{aligned} \quad (3.8)$$

illustrates both sets. As the explicit relations similar to those of (3.6) are not required for the present computation we have not determined them here.

Having established the mapping of the evanescent \mathbb{C}_{qrs} structures to the four dimensional ones these are applied to the evaluation of the Green's function *before* the renormalization constant for $\mathcal{O}_{\alpha\beta\gamma}^{ijk}$ is extracted in the $\overline{\text{MS}}$ scheme [12, 13]. In other words the ϵ expansion of the d -dependent coefficients of each term in (3.6) is effected first. This results in the four dimensional anomalous dimension

$$\begin{aligned} \gamma_{\mathcal{O}}(a) = & \frac{1}{3} \mathbb{C}_{220} a + \left[[4N_f - 72] \mathbb{C}_{000} + \left[\frac{47}{18} - \frac{1}{27} N_f \right] \mathbb{C}_{220} + \frac{1}{36} \mathbb{C}_{220}^2 - \frac{5}{36} \mathbb{C}_{440} \right] a^2 \\ & + \left[\left[\frac{1706}{9} N_f - 34\zeta_3 - \frac{16094}{9} - \frac{20}{9} N_f^2 \right] \mathbb{C}_{000} \right. \\ & + \left[\frac{5873}{108} - \frac{433}{18} \zeta_3 - \frac{71}{27} N_f - \frac{40}{9} \zeta_3 N_f - \frac{13}{81} N_f^2 \right] \mathbb{C}_{220} + \left[\frac{5}{648} - \frac{1}{27} \zeta_3 \right] \mathbb{C}_{220}^3 \\ & + \left[\frac{1}{324} N_f - \frac{209}{324} + \frac{71}{27} \zeta_3 \right] \mathbb{C}_{220}^2 + \left[\frac{25}{144} \zeta_3 - \frac{37}{432} \right] \mathbb{C}_{220} \mathbb{C}_{440} \\ & + \left[\frac{91}{72} - \frac{29}{12} \zeta_3 + \frac{7}{324} N_f \right] \mathbb{C}_{440} + \left[\frac{2}{9} \zeta_3 - \frac{1}{8} \right] \mathbb{C}_{444} \left. \right] a^3 \\ & + \left[\left[\frac{523475}{81} N_f - 120\zeta_5 N_f - 34\zeta_4 N_f + 561\zeta_4 - \frac{392305}{9} - \frac{11417}{81} N_f^2 - \frac{160}{3} \zeta_3 N_f^2 \right. \right. \\ & \left. \left. - \frac{140}{81} N_f^3 + \frac{227}{27} \zeta_3 + \frac{5918}{9} \zeta_3 N_f + \frac{412390}{27} \zeta_5 \right] \mathbb{C}_{000} \right. \\ & + \left[\frac{2252615}{1944} - \frac{328151}{324} \zeta_3 - \frac{146083}{972} N_f - \frac{6463}{27} \zeta_3 N_f - \frac{40}{9} \zeta_4 N_f^2 - \frac{5}{27} N_f^3 + \frac{16}{81} \zeta_3 N_f^3 \right. \\ & \left. + \frac{440}{81} \zeta_3 N_f^2 + \frac{887}{18} \zeta_4 N_f + \frac{1853}{1458} N_f^2 + \frac{4763}{12} \zeta_4 + \frac{5620}{27} \zeta_5 N_f + \frac{145675}{324} \zeta_5 \right] \mathbb{C}_{220} \\ & + \left[\frac{42383}{1296} + \frac{200135}{1944} \zeta_3 - \frac{208495}{972} \zeta_5 - \frac{5743}{5832} N_f - \frac{1507}{972} \zeta_3 N_f - \frac{781}{18} \zeta_4 - \frac{37}{1458} N_f^2 \right. \\ & \left. - \frac{20}{9} \zeta_5 N_f + \frac{71}{27} \zeta_4 N_f \right] \mathbb{C}_{220}^2 \\ & + \left[\frac{7}{11664} N_f - \frac{9821}{7776} - \frac{1}{27} \zeta_4 N_f + \frac{5}{243} \zeta_3 N_f + \frac{11}{18} \zeta_4 + \frac{2183}{3888} \zeta_3 + \frac{4205}{1944} \zeta_5 \right] \mathbb{C}_{220}^3 \\ & + \left[\frac{929}{15552} \zeta_3 - \frac{605}{15552} \zeta_5 - \frac{101}{31104} \right] \mathbb{C}_{220}^4 + \left[\frac{1015}{7776} \zeta_5 - \frac{2105}{15552} \zeta_3 - \frac{13}{576} \right] \mathbb{C}_{220}^2 \mathbb{C}_{440} \\ & + \left[\frac{2669}{972} + \frac{5513}{648} \zeta_3 - \frac{16165}{864} \zeta_5 - \frac{275}{96} \zeta_4 - \frac{125}{1296} \zeta_3 N_f - \frac{11}{324} N_f + \frac{25}{144} \zeta_4 N_f \right] \mathbb{C}_{220} \mathbb{C}_{440} \\ & + \left[\frac{173105}{648} \zeta_5 - \frac{98657}{1296} - \frac{75593}{648} \zeta_3 - \frac{29}{12} \zeta_4 N_f + \frac{5}{9} \zeta_5 N_f + \frac{319}{8} \zeta_4 + \frac{373}{2916} N_f^2 \right. \\ & \left. + \frac{679}{162} \zeta_3 N_f + \frac{2603}{972} N_f \right] \mathbb{C}_{440} + \left[\frac{895}{1944} \zeta_5 - \frac{2009}{3888} \zeta_3 - \frac{65}{1296} \right] \mathbb{C}_{444} \mathbb{C}_{220} \\ & + \left[\frac{6721}{648} - \frac{48235}{1296} \zeta_5 - \frac{18419}{1296} \zeta_3 - \frac{11}{3} \zeta_4 - \frac{11}{81} N_f + \frac{1}{54} \zeta_3 N_f + \frac{2}{9} \zeta_4 N_f \right] \mathbb{C}_{444} \end{aligned}$$

$$+ \left[\frac{865}{31104} - \frac{1025}{15552} \zeta_5 - \frac{235}{15552} \zeta_3 \right] \mathbb{C}_{440}^2 \Big] a^4 + O(a^5) \quad (3.9)$$

to four loops or

$$\begin{aligned} \gamma_{\mathcal{O}}(a) = & \left[0.333333a + (2.611111 - 0.037037N_f)a^2 + (25.463483 - 0.160494N_f^2 - 7.972105N_f)a^3 \right. \\ & \left. + (0.052258N_f^3 + 2.990285N_f^2 - 168.858883N_f + 837.104813)a^4 \right] \mathbb{C}_{220} \\ & + \left[(4.000000N_f - 72.000000)a^2 + (-2.222222N_f^2 + 189.555556N_f - 1829.092157)a^3 \right. \\ & \left. + (-1.728395N_f^3 - 205.060319N_f^2 + 7091.843195N_f - 27134.427634)a^4 \right] \mathbb{C}_{000} \\ & + \left[-0.138889a^2 + (0.021605N_f - 1.6410819)a^3 \right. \\ & \left. + (0.127915N_f^2 + 5.676691N_f + 103.808552)a^4 \right] \mathbb{C}_{440} \\ & + \left[0.027778a^2 + (0.003086N_f + 2.515903)a^3 \right. \\ & \left. + (-0.025377N_f^2 - 2.306597N_f - 112.9280589)a^4 \right] \mathbb{C}_{220}^2 \\ & + \left[0.142124a^3 + (0.126974N_f - 49.273223)a^4 \right] \mathbb{C}_{444} \\ & + \left[0.123042a^3 + (0.038014N_f - 9.528152)a^4 \right] \mathbb{C}_{220}\mathbb{C}_{440} \\ & + \left[-0.036805a^3 + (-0.014752N_f + 2.316294)a^4 \right] \mathbb{C}_{220}^3 \\ & + \left[0.028219\mathbb{C}_{220}^4 - 0.058696\mathbb{C}_{440}^2 - 0.193887\mathbb{C}_{444}\mathbb{C}_{220} - 0.049921\mathbb{C}_{220}^2\mathbb{C}_{440} \right] a^4 \\ & + O(a^5) \end{aligned} \quad (3.10)$$

numerically. One observation deserves comment and it concerns the comparison of the results of (3.2) with (3.9). If one formally replaces the \mathbb{C}_{qrs} matrices in (3.2) with their strictly four dimensional counterparts then (3.9) is reproduced. By this we mean the evanescent matrices of (3.2) are replaced using the relations of (3.5) and (3.6) but with d replaced by 4. This is consistent with the general formal relation

$$\gamma_{\mathcal{O}}(a) = \lim_{d \rightarrow 4} \gamma_{\mathcal{O}}^{\text{naive}}(a) \quad (3.11)$$

which additionally provides a check on the translation of the two actual renormalization constants into their respective $\overline{\text{MS}}$ anomalous dimensions. It is worth recalling that the \mathbb{C}_{qrs} structures that remain in (3.9) are, [12, 13],

$$\begin{aligned} \mathbb{C}_{000} \Big|_{d=4} &= \mathcal{I} \otimes \mathcal{I} \otimes \mathcal{I} \\ \mathbb{C}_{220} \Big|_{d=4} &= \sigma^{\mu\nu} \otimes \sigma_{\mu\nu} \otimes \mathcal{I} + \sigma^{\mu\nu} \otimes \mathcal{I} \otimes \sigma_{\mu\nu} + \mathcal{I} \otimes \sigma^{\mu\nu} \otimes \sigma_{\mu\nu} \\ \mathbb{C}_{440} \Big|_{d=4} &= 24 [\gamma^5 \otimes \gamma^5 \otimes \mathcal{I} + \gamma^5 \otimes \mathcal{I} \otimes \gamma^5 + \mathcal{I} \otimes \gamma^5 \otimes \gamma^5] \\ \mathbb{C}_{444} \Big|_{d=4} &= 0 \end{aligned} \quad (3.12)$$

in four dimensions.

Spin	Chirality	\mathbb{C}_{000}	\mathbb{C}_{220}	\mathbb{C}_{440}	\mathbb{C}_{444}
$(\frac{1}{2}, 0)$	+	1	12	72	0
$(\frac{1}{2}, 0)$	-	1	12	-24	0
$(\frac{3}{2}, 0)$	+	1	-12	72	0
$(1, \frac{1}{2})$	-	1	-4	-24	0

Table 1: Values for the evaluation of the general anomalous dimension for various nucleons.

The main application of (3.9) is to extract anomalous dimensions for four core baryon operators which are central to the evaluation of nucleon matrix elements. These were introduced in [11, 34] and defined by

$$\begin{aligned}\mathcal{O}_+^{(\frac{1}{2},0)} &= \epsilon^{IJK} \psi_L^I \left((\psi_L^J)^T C \psi_L^K \right) \quad , \quad \mathcal{O}_-^{(\frac{1}{2},0)} = \epsilon^{IJK} \psi_R^I \left((\psi_L^J)^T C \psi_L^K \right) \\ \mathcal{O}_+^{(\frac{3}{2},0)} &= \epsilon^{IJK} \Delta \psi_L^I \Delta \psi_L^J \Delta \psi_L^K \quad , \quad \mathcal{O}_-^{(1,\frac{1}{2})} = \epsilon^{IJK} \Delta \psi_L^I \Delta \psi_L^J \Delta \psi_R^K\end{aligned}\quad (3.13)$$

where $\Delta^2 = 0$. The right and left handed quarks are denoted by $\psi_R = \frac{1}{2}(1+\gamma^5)\psi$ and $\psi_L = \frac{1}{2}(1-\gamma^5)\psi$ respectively, the first superscript represents the spin that is not part of the bilinear part of the operator and the second relates to the bilinear properties itself, and the subscript sign indicates the chirality [12, 20]. For more details on the discrete and continuous symmetries of these operators see the discussion in [20]. To extract the respective anomalous dimensions merely requires substituting the eigenvalues of the respective \mathbb{C}_{grs} structures that were deduced in [12, 20, 35] and recorded in Table 1. Consequently we have

$$\begin{aligned}\gamma_+^{(\frac{1}{2},0)}(a) &= 4a + \left[\frac{32}{9} N_f - \frac{140}{3} \right] a^2 + \left[160 N_f - 32 \zeta_3 - \frac{10784}{9} - \frac{160}{3} \zeta_3 N_f - \frac{112}{27} N_f^2 \right] a^3 \\ &+ \left[528 \zeta_4 + 848 \zeta_4 N_f - \frac{4928575}{162} - \frac{86600}{27} \zeta_5 - \frac{58972}{27} \zeta_3 N_f - \frac{29195}{243} N_f^2 - \frac{320}{81} N_f^3 \right. \\ &\quad \left. - \frac{160}{3} \zeta_4 N_f^2 + \frac{64}{27} \zeta_3 N_f^3 + \frac{320}{27} \zeta_3 N_f^2 + \frac{18880}{9} \zeta_5 N_f + \frac{63670}{27} \zeta_3 + \frac{379232}{81} N_f \right] a^4 \\ &+ O(a^5) \\ \gamma_-^{(\frac{1}{2},0)}(a) &= 4a + \left[\frac{32}{9} N_f - \frac{100}{3} \right] a^2 + \left[\frac{4264}{27} N_f - \frac{10988}{9} - \frac{160}{3} \zeta_3 N_f - \frac{112}{27} N_f^2 \right] a^3 \\ &+ \left[880 \zeta_4 N_f - 8800 \zeta_5 - \frac{4227355}{162} - \frac{66836}{27} \zeta_3 N_f - \frac{32179}{243} N_f^2 - \frac{320}{81} N_f^3 - \frac{160}{3} \zeta_4 N_f^2 \right. \\ &\quad \left. + \frac{64}{27} \zeta_3 N_f^3 + \frac{320}{27} \zeta_3 N_f^2 + \frac{18400}{9} \zeta_5 N_f + \frac{153818}{27} \zeta_3 + \frac{361576}{81} N_f \right] a^4 + O(a^5) \\ \gamma_+^{(\frac{3}{2},0)}(a) &= -4a + \left[\frac{40}{9} N_f - \frac{328}{3} \right] a^2 + \left[\frac{2008}{9} N_f - 2382 - \frac{8}{27} N_f^2 + \frac{160}{3} \zeta_3 N_f + \frac{1120}{3} \zeta_3 \right] a^3 \\ &+ \left[\frac{40}{81} N_f^3 - 6160 \zeta_4 - \frac{9495365}{162} - \frac{36607}{243} N_f^2 - \frac{26080}{9} \zeta_5 N_f - \frac{3200}{27} \zeta_3 N_f^2 - \frac{1520}{3} \zeta_4 N_f \right. \\ &\quad \left. - \frac{64}{27} \zeta_3 N_f^3 + \frac{160}{3} \zeta_4 N_f^2 + \frac{98720}{27} \zeta_3 N_f + \frac{270644}{27} \zeta_3 + \frac{293120}{27} \zeta_5 + \frac{675982}{81} N_f \right] a^4 \\ &+ O(a^5) \\ \gamma_-^{(1,\frac{1}{2})}(a) &= -\frac{4}{3} a + \left[\frac{112}{27} N_f - \frac{236}{3} \right] a^2 + \left[\frac{160}{9} \zeta_3 N_f + \frac{544}{3} \zeta_3 + \frac{16168}{81} N_f - \frac{18496}{9} - \frac{128}{81} N_f^2 \right] a^3 \\ &+ \left[\frac{565420}{81} N_f - 2992 \zeta_4 - 112 \zeta_4 N_f - \frac{22115885}{486} - \frac{36331}{243} N_f^2 - \frac{27040}{27} \zeta_5 N_f \right. \\ &\quad \left. - \frac{6080}{81} \zeta_3 N_f^2 - \frac{80}{81} N_f^3 - \frac{64}{81} \zeta_3 N_f^3 + \frac{160}{9} \zeta_4 N_f^2 + \frac{119804}{81} \zeta_3 N_f + \frac{388640}{243} \zeta_5 \right. \\ &\quad \left. + \frac{2271070}{243} \zeta_3 \right] a^4 + O(a^5)\end{aligned}\quad (3.14)$$

where we reproduced the lower loop results of [11, 12, 13] which represents a minor check since [13] did not use FORCER. Another check is provided by the large N_f result of [36] where the coefficients of the leading order N_f terms of $\gamma_{\pm}^{(\frac{1}{2},0)}(a)$ were computed. It is therefore reassuring to note the

coefficient of N_f^3 in the four loop term of both these anomalous dimensions is in agreement with the second expression of equation (21) in [36]. Numerically we have

$$\begin{aligned}
\gamma_+^{(\frac{1}{2},0)}(a) &= 4.000000a + (3.555556N_f - 46.666667)a^2 \\
&\quad + (-4.148148N_f^2 + 95.890298N_f - 1236.688043)a^3 \\
&\quad + (-1.101297N_f^3 - 163.621338N_f^2 + 5149.460288N_f - 30343.057304)a^4 + O(a^5) \\
\gamma_-^{(\frac{1}{2},0)}(a) &= 4.000000a + (3.555556N_f - 33.333333)a^2 \\
&\quad + (-4.148148N_f^2 + 93.8162244N_f - 1220.888889)a^3 \\
&\quad + (-1.101297N_f^3 - 175.901174N_f^2 + 4560.706306N_f - 28371.674539)a^4 + O(a^5) \\
\gamma_+^{(\frac{3}{2},0)}(a) &= -4.000000a + (4.444444N_f - 109.333333)a^2 \\
&\quad + (-0.296296N_f^2 + 287.220813N_f - 1933.232089)a^3 \\
&\quad + (-2.355493N_f^3 - 235.388188N_f^2 + 9187.369682N_f - 41974.040055)a^4 + O(a^5) \\
\gamma_-^{(1,\frac{1}{2})}(a) &= -1.333333a + (4.148148N_f - 78.666667)a^2 \\
&\quad + (-1.580247N_f^2 + 220.974839N_f - 1837.138126)a^3 \\
&\quad + (-1.937428N_f^3 - 220.497455N_f^2 + 7598.726041N_f - 35851.461429)a^4 \\
&\quad + O(a^5)
\end{aligned} \tag{3.15}$$

in the $\overline{\text{MS}}$ scheme.

4 Banks-Zaks fixed point.

As an application of our baryon operator anomalous dimensions we examine them at the Banks-Zaks fixed point [26, 37]. This is a fixed point in the situation where the two loop term of the β -function for a non-abelian asymptotically free gauge theory is positive. It defines the conformal window. From the $SU(3)$ two loop β -function the window lies in the range $8 < N_f \leq 16$. The lower boundary is determined from the two loop term and there has been a long debate as to whether that boundary remains there when non-perturbative contributions are included. However a technique was introduced in [26] where perturbation theory is carried out in terms of a purely dimensionless N_f dependent parameter that allows one to compute critical exponents of anomalous dimensions. In our $SU(3)$ case we take

$$\Delta_{\text{BZ}} = 11 - \frac{2}{3}N_f \tag{4.1}$$

as our convention for this parameter. The leading order Banks-Zaks critical coupling constant is determined by redefining N_f in the two loop β -function using (4.1) and finding the non-trivial solution of $\beta(a) = 0$ as a function of Δ_{BZ} . Corrections to the leading order critical coupling a_{BZ} are deduced by including the high order terms in the β -function. As we have determined the baryon dimensions to four loops this means we need the five loop β -function to deduce the fourth order term in the associated critical exponents. The reason for this is that the one and two loop terms are used to determine the leading term of a_{BZ} . Consequently for $SU(3)$ we find

$$\begin{aligned}
a_{\text{BZ}} &= \frac{\Delta_{\text{BZ}}}{107} + \frac{11675}{29401032}\Delta_{\text{BZ}}^2 + [219204480\zeta_3 + 145645559]\frac{\Delta_{\text{BZ}}^3}{1346449661472} \\
&\quad + [158627906059008\zeta_3 - 242692714598400\zeta_5 + 119816461287557]\frac{\Delta_{\text{BZ}}^4}{6659496939251344896} \\
&\quad + O(\Delta_{\text{BZ}}^5) .
\end{aligned} \tag{4.2}$$

Using this value we can deduce the anomalous dimension of the general operator at the Banks-Zaks fixed point which is

$$\begin{aligned}
\gamma_{\mathcal{O}(a_{\text{BZ}})} = & \left[\frac{1}{321} \Delta_{\text{BZ}} + \frac{27083}{88203096} \Delta_{\text{BZ}}^2 + \left[\frac{352124197}{12118046953248} - \frac{59531}{2359432818} \zeta_3 \right] \Delta_{\text{BZ}}^3 \right. \\
& + \left. \left[\frac{21882082084039}{6659496939251344896} + \frac{79450145}{4544267607468} \zeta_5 - \frac{20367037045}{1944946535996304} \zeta_3 \right] \Delta_{\text{BZ}}^4 \right] \mathbb{C}_{220} \\
& + \left[-\frac{6}{11449} \Delta_{\text{BZ}}^2 + \left[\frac{72973}{2359432818} - \frac{34}{1225043} \zeta_3 \right] \Delta_{\text{BZ}}^3 \right. \\
& + \left. \left[\frac{7103828059}{1296631023997536} - \frac{75332681}{1514755869156} \zeta_3 + \frac{358930}{3539149227} \zeta_5 \right] \Delta_{\text{BZ}}^4 \right] \mathbb{C}_{000} \\
& + \left[\frac{1}{412164} \Delta_{\text{BZ}}^2 + \left[\frac{71}{33076161} \zeta_3 - \frac{47365}{169879162896} \right] \Delta_{\text{BZ}}^3 \right. \\
& + \left. \left[\frac{6326616091}{93357433727822592} + \frac{25858273}{27265605644808} \zeta_3 - \frac{244135}{127409372172} \zeta_5 \right] \Delta_{\text{BZ}}^4 \right] \mathbb{C}_{220}^2 \\
& + \left[-\frac{5}{412164} \Delta_{\text{BZ}}^2 + \left[\frac{16525}{56626387632} - \frac{29}{14700516} \zeta_3 \right] \Delta_{\text{BZ}}^3 \right. \\
& + \left. \left[\frac{179045}{84939581448} \zeta_5 - \frac{4311271033}{31119144575940864} - \frac{37679737}{36354140859744} \zeta_3 \right] \Delta_{\text{BZ}}^4 \right] \mathbb{C}_{440} \\
& + \left[\left[\frac{5}{793827864} - \frac{1}{33076161} \zeta_3 \right] \Delta_{\text{BZ}}^3 \right. \\
& + \left. \left[\frac{4205}{254818744344} \zeta_5 + \frac{164671}{54531211289616} \zeta_3 - \frac{636697}{72708281719488} \right] \Delta_{\text{BZ}}^4 \right] \mathbb{C}_{220}^3 \\
& + \left[\left[\frac{25}{176406192} \zeta_3 - \frac{37}{529218576} \right] \Delta_{\text{BZ}}^3 \right. \\
& + \left. \left[\frac{3386513}{436249690316928} + \frac{10299631}{145416563438976} \zeta_3 - \frac{16165}{113252775264} \zeta_5 \right] \Delta_{\text{BZ}}^4 \right] \mathbb{C}_{220} \mathbb{C}_{440} \\
& + \left[\left[\frac{2}{11025387} \zeta_3 - \frac{1}{9800344} \right] \Delta_{\text{BZ}}^3 \right. \\
& + \left. \left[\frac{3564589}{72708281719488} - \frac{1508161}{18177070429872} \zeta_3 - \frac{48235}{169879162896} \zeta_5 \right] \Delta_{\text{BZ}}^4 \right] \mathbb{C}_{444} \\
& + \left[\left[\frac{929}{2038549954752} \zeta_3 - \frac{605}{2038549954752} \zeta_5 - \frac{101}{4077099909504} \right] \mathbb{C}_{220}^4 \right. \\
& + \left[\frac{1015}{1019274977376} \zeta_5 - \frac{2105}{2038549954752} \zeta_3 - \frac{13}{75501850176} \right] \mathbb{C}_{220}^2 \mathbb{C}_{440} \\
& + \left[\frac{895}{254818744344} \zeta_5 - \frac{2009}{509637488688} \zeta_3 - \frac{65}{169879162896} \right] \mathbb{C}_{444} \mathbb{C}_{220} \\
& + \left. \left[\frac{865}{4077099909504} - \frac{1025}{2038549954752} \zeta_5 - \frac{235}{2038549954752} \zeta_3 \right] \mathbb{C}_{440}^2 \right] \Delta_{\text{BZ}}^4 \\
& + O(\Delta_{\text{BZ}}^5)
\end{aligned} \tag{4.3}$$

or

$$\begin{aligned}
\gamma_{\mathcal{O}(a_{\text{BZ}})} = & 3.115265 \times 10^{-3} \mathbb{C}_{220} \Delta_{\text{BZ}} \\
& + [-5.240632 \times 10^{-4} \mathbb{C}_{000} + 2.426219 \times 10^{-6} \mathbb{C}_{220}^2 + 3.070527 \times 10^{-4} \mathbb{C}_{220} \\
& - 1.213109 \times 10^{-5} \mathbb{C}_{440}] \Delta_{\text{BZ}}^2 \\
& + [-2.433845 \times 10^{-6} \mathbb{C}_{000} - 3.004350 \times 10^{-8} \mathbb{C}_{220}^3 + 2.301473 \times 10^{-6} \mathbb{C}_{220}^2
\end{aligned}$$

$$\begin{aligned}
& +1.004392 \times 10^{-7} \mathbb{C}_{220} \mathbb{C}_{440} - 1.271340 \times 10^{-6} \mathbb{C}_{220} - 2.079496 \times 10^{-6} \mathbb{C}_{440} \\
& + 1.160153 \times 10^{-7} \mathbb{C}_{444} \Delta_{\text{BZ}}^3 \\
& + [5.085945 \times 10^{-5} \mathbb{C}_{000} + 2.152852 \times 10^{-10} \mathbb{C}_{220}^4 + 1.198435 \times 10^{-8} \mathbb{C}_{220}^3 \\
& - 3.808425 \times 10^{-10} \mathbb{C}_{220}^2 \mathbb{C}_{440} - 7.791257 \times 10^{-7} \mathbb{C}_{220}^2 - 5.510202 \times 10^{-8} \mathbb{C}_{220} \mathbb{C}_{440} \\
& - 1.479153 \times 10^{-9} \mathbb{C}_{444} \mathbb{C}_{220} + 8.827407 \times 10^{-6} \mathbb{C}_{220} - 4.477861 \times 10^{-10} \mathbb{C}_{440}^2 \\
& + 8.013217 \times 10^{-7} \mathbb{C}_{440} - 3.451317 \times 10^{-7} \mathbb{C}_{444}] \Delta_{\text{BZ}}^4 + O(\Delta_{\text{BZ}}^5). \tag{4.4}
\end{aligned}$$

numerically. Consequently the anomalous dimensions of the four core baryon operators are

$$\begin{aligned}
\gamma_+^{(\frac{1}{2},0)}(a_{\text{BZ}}) &= \frac{4}{107} \Delta_{\text{BZ}} + \frac{19379}{7350258} \Delta_{\text{BZ}}^2 + \left[\frac{314021069}{1009837246104} - \frac{12224}{131079601} \zeta_3 \right] \Delta_{\text{BZ}}^3 \\
&+ \left[\frac{19461603055087}{554958078270945408} - \frac{1981080112}{40519719499923} \zeta_3 + \frac{35529320}{378688967289} \zeta_5 \right] \Delta_{\text{BZ}}^4 \\
&+ O(\Delta_{\text{BZ}}^5) \\
\gamma_-^{(\frac{1}{2},0)}(a_{\text{BZ}}) &= \frac{4}{107} \Delta_{\text{BZ}} + \frac{9313}{2450086} \Delta_{\text{BZ}}^2 + \left[\frac{40784885}{112204138456} - \frac{8800}{131079601} \zeta_3 \right] \Delta_{\text{BZ}}^3 \\
&+ \left[\frac{22658041606303}{554958078270945408} - \frac{218534068}{13506573166641} \zeta_3 + \frac{1870000}{42076551921} \zeta_5 \right] \Delta_{\text{BZ}}^4 \\
&+ O(\Delta_{\text{BZ}}^5) \\
\gamma_+^{(\frac{3}{2},0)}(a_{\text{BZ}}) &= -\frac{4}{107} \Delta_{\text{BZ}} - \frac{34787}{7350258} \Delta_{\text{BZ}}^2 + \left[\frac{146240}{393238803} \zeta_3 - \frac{32245429}{112204138456} \right] \Delta_{\text{BZ}}^3 \\
&+ \left[\frac{2820290956}{40519719499923} \zeta_3 - \frac{51566480}{378688967289} \zeta_5 - \frac{14951711813983}{554958078270945408} \right] \Delta_{\text{BZ}}^4 \\
&+ O(\Delta_{\text{BZ}}^5) \\
\gamma_-^{(1,\frac{1}{2})}(a_{\text{BZ}}) &= -\frac{4}{321} \Delta_{\text{BZ}} - \frac{31363}{22050774} \Delta_{\text{BZ}}^2 + \left[\frac{22336}{131079601} \zeta_3 - \frac{314714429}{3029511738312} \right] \Delta_{\text{BZ}}^3 \\
&+ \left[\frac{14316089632}{364677475499307} \zeta_3 - \frac{222460400}{3408200705601} \zeta_5 - \frac{109005718637}{61662008696771712} \right] \Delta_{\text{BZ}}^4 \\
&+ O(\Delta_{\text{BZ}}^5). \tag{4.5}
\end{aligned}$$

Expressing these numerically leads to

$$\begin{aligned}
\gamma_+^{(\frac{1}{2},0)}(a_{\text{BZ}}) &= 3.738318 \times 10^{-2} \Delta_{\text{BZ}} + 2.636506 \times 10^{-3} \Delta_{\text{BZ}}^2 + 1.988627 \times 10^{-4} \Delta_{\text{BZ}}^3 \\
&+ 7.358447 \times 10^{-5} \Delta_{\text{BZ}}^4 + O(\Delta_{\text{BZ}}^5) \\
\gamma_-^{(\frac{1}{2},0)}(a_{\text{BZ}}) &= 3.738318 \times 10^{-2} \Delta_{\text{BZ}} + 3.801091 \times 10^{-3} \Delta_{\text{BZ}}^2 + 2.827884 \times 10^{-4} \Delta_{\text{BZ}}^3 \\
&+ 6.746328 \times 10^{-5} \Delta_{\text{BZ}}^4 + O(\Delta_{\text{BZ}}^5) \\
\gamma_+^{(\frac{3}{2},0)}(a_{\text{BZ}}) &= -3.738318 \times 10^{-2} \Delta_{\text{BZ}} - 4.732759 \times 10^{-3} \Delta_{\text{BZ}}^2 + 1.596463 \times 10^{-4} \Delta_{\text{BZ}}^3 \\
&- 8.447494 \times 10^{-5} \Delta_{\text{BZ}}^4 + O(\Delta_{\text{BZ}}^5) \\
\gamma_-^{(1,\frac{1}{2})}(a_{\text{BZ}}) &= -1.246106 \times 10^{-2} \Delta_{\text{BZ}} - 1.422308 \times 10^{-3} \Delta_{\text{BZ}}^2 + 1.009479 \times 10^{-4} \Delta_{\text{BZ}}^3 \\
&- 2.226127 \times 10^{-5} \Delta_{\text{BZ}}^4 + O(\Delta_{\text{BZ}}^5) \tag{4.6}
\end{aligned}$$

from which it can be observed that the coefficients of each operator dimension diminish by roughly an order of magnitude with respect to this expansion parameter. Moreover as Δ_{BZ} ranges from $1/3$ to $17/3$ for $N_f = 16$ down to $N_f = 8$ across the conformal window it may appear that the series convergence should be reasonable. In order to gauge this we have plotted the anomalous

dimensions for each of the operators in Figure 3 for the leading order (LO) to the fourth order term which is next-to-next-to-next-to leading order (NNNLO). We note the leading order is linear in N_f and so has a limited contribution to the convergence discussion.

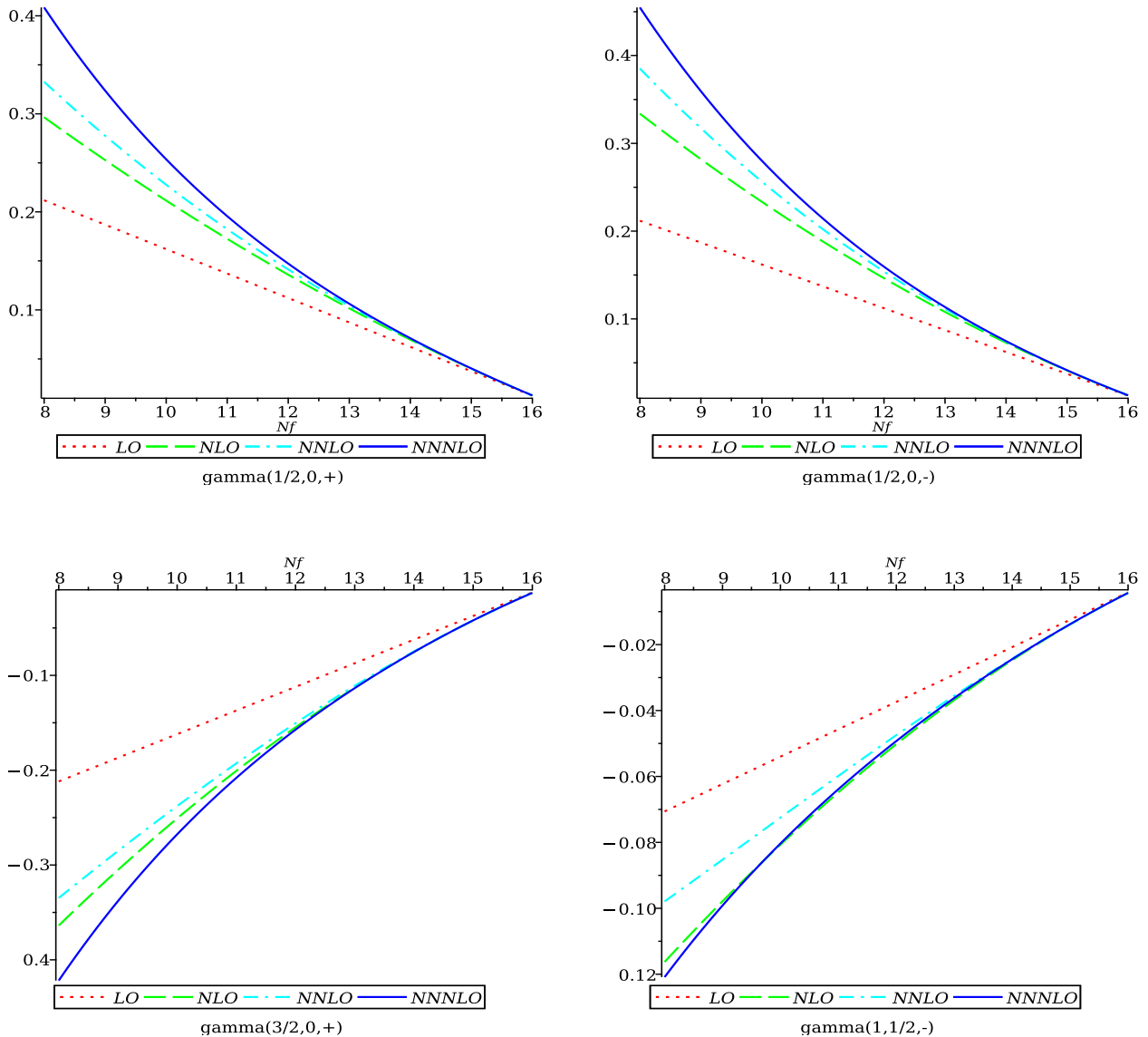


Figure 3: Plots of the leading order (LO), next-to-leading order (NLO), next-to-next-to-leading order (NNLO), next-to-next-to-next-to-leading order (NNNLO), anomalous dimension of the four baryon operators at the Banks-Zaks fixed point for $8 \leq N_f \leq 16$.

What is evident from Figure 3 is that for each of the four operators perturbation theory appears to be reliable down to around $N_f = 12$. While if anything it may seem that the behaviour of the two spin- $\frac{1}{2}$ cases are both less accurate at this value than either the spin-1 or spin- $\frac{3}{2}$ operator dimensions this is not the case. Examining the lower plots of Figure 3 there is a wide fluctuation below $N_f = 12$ since the second and fourth order lines are particularly close especially in the spin-1 situation. This contrasts with the spin- $\frac{1}{2}$ plots where there is no fluctuation of the order. In order to explore the convergence of each series we have undertaken a Padé approximant study on the fourth order expression which will provide three examples. This is because the leading order

is $O(\Delta_{\text{BZ}})$. So we will construct the $[1, 1]$, $[1, 2]$ and $[2, 2]$ approximants from the second, third and fourth order approximations. The numerical values of the resulting exponents are provided in Table 2. It is clear that the convergence for the two spin- $\frac{1}{2}$ operators is improved for $N_f \leq 12$ and particularly so for the positive chirality case even for $N_f = 8$. Though in this specific case the situation has to be qualified by noting that this value of N_f may be outside the actual conformal window. As yet there has been no definitive determination as to what that value is. To understand these comments further and to illustrate the improvement provided by the Padé approximant we have plotted the graphs of the three approximants of each of the two spin- $\frac{1}{2}$ operators in Figure 4. The distinctly more accurate convergence in the positive chirality case is apparent. For the remaining two operators the convergence of both their approximants appear not to have improved below $N_f = 14$ which is why we have not provided any illustrations of those approximants. In essence the order-by-order discrepancies in Table 2 is a reflection of this. Finally we note that the respective unitarity bounds of each of the operators, which were derived in [20] and checked to third order, remain unviolated at fourth order in the conformal window range.

Exponent	N_f	$P_{[1,1]}$	$P_{[1,2]}$	$P_{[2,2]}$
$\gamma_+^{(\frac{1}{2},0)}(a_{\text{BZ}})$	8	0.352858	0.359503	0.352594
	10	0.233291	0.235492	0.233174
	12	0.142246	0.142809	0.142201
	14	0.070604	0.070681	0.070593
	16	0.012761	0.012761	0.012760
$\gamma_-^{(\frac{1}{2},0)}(a_{\text{BZ}})$	8	0.499833	0.413023	0.472906
	10	0.289590	0.264920	0.281032
	12	0.161375	0.155779	0.159019
	14	0.075018	0.074329	0.074632
	16	0.012898	0.012894	0.012895
$\gamma_+^{(\frac{3}{2},0)}(a_{\text{BZ}})$	8	-0.749623	-0.226711	-0.389838
	10	-0.358874	-0.194575	-0.257553
	12	-0.180829	-0.139684	-0.155322
	14	-0.078968	-0.073701	-0.075236
	16	-0.013010	-0.012980	-0.012982
$\gamma_-^{(1,\frac{1}{2})}(a_{\text{BZ}})$	8	-0.199920	-0.068444	-0.110503
	10	-0.106844	-0.059855	-0.077264
	12	-0.056850	-0.044097	-0.048697
	14	-0.025647	-0.023914	-0.024388
	16	-0.004318	-0.004307	-0.004308

Table 2: Padé estimates for the anomalous dimension of the four baryon operators at the Banks-Zaks fixed point for $8 \leq N_f \leq 16$.

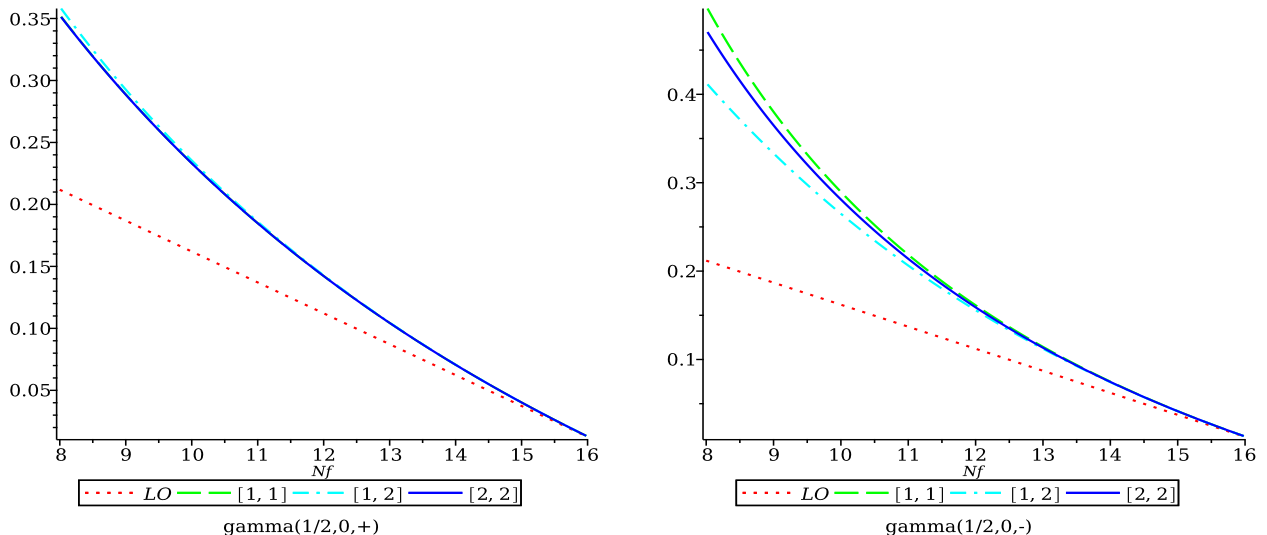


Figure 4: Plots of the Padé estimates for the anomalous dimension of the two spin- $\frac{1}{2}$ baryon operators at the Banks-Zaks fixed point for $8 \leq N_f \leq 16$.

5 Discussion.

We have completed the four loop $\overline{\text{MS}}$ scheme renormalization of a general 3-quark operator using the Manashov and Kränkl approach thereby extending the two and three loop results of [12, 13]. In carrying out the renormalization with a general and flexible approach the anomalous dimensions of several baryonic bound states have been deduced as a by-product. Since such baryon operators have been of interest in exploring ideas for extensions of the Standard Model, [19, 20, 21, 22, 23, 24, 25], by way of an application we examined the behaviour of the eigen-operator anomalous dimensions in the conformal window of QCD using Banks-Zaks perturbation theory, [26]. Ordinarily from similar studies, such as [38] for example, perturbation theory is reliable from the top of the window down to around about $N_f = 12$. By this we mean that the leading, next-to-leading, next-to-next-to-leading and next-to-next-to-next-to-leading approximations produce critical exponent estimates that are in close agreement. Below this value of N_f , where the Banks-Zaks fixed point starts to drift beyond the perturbative approximation, the estimates begin to diverge. What was interesting with several of the baryon operator critical exponents was that Padé approximants appeared to improve the convergence down to the neighbourhood of what is perceived to be the lower conformal window boundary. However this was very much dependent on the actual operator itself rather than being a global property. What would be interesting to ascertain is whether the Padé estimates of the $\mathcal{O}_+^{(\frac{1}{2},0)}$ and $\mathcal{O}_-^{(\frac{1}{2},0)}$ dimensions could be measured using lattice field theory for $N_f = 10$ for instance. The reason being that from lattice field theory studies this N_f value is believed to lie inside the conformal window. If so it would give momentum to following a similar approach for other useful operators in conformal window analyses of Standard Model extensions. Separately another thread that needs to be followed is to extend the evaluation of baryon operator dimensions to the determination of their higher moments.

Data Availability Statement. The data that support the findings of this article are openly available [39].

Acknowledgement. The author thanks the DESY Zeuthen theory group, where part of this work was carried out, for their hospitality and Kolleg Mathematik Physik Berlin for a Visiting Scholarship. We thank L. Vecchi for correspondence. The research was carried out with the support of the STFC Consolidated Grant ST/X000699/1 and was undertaken on BARKLA, part of the High Performance Computing facilities at the University of Liverpool, UK. For the purpose of open access, the author has applied a Creative Commons Attribution (CC-BY) licence to any Author Accepted Manuscript version arising.

A Products of \mathbb{C}_{qrs} .

In this appendix we record the products of \mathbb{C}_{qrs} which were required to convert the operator renormalization constant to its anomalous dimension in (3.1). We have

$$\begin{aligned}
\mathbb{C}_{220}\mathbb{C}_{220} &= 6d(d-1)\mathbb{C}_{000} + 4(d-3)\mathbb{C}_{220} + \mathbb{C}_{440} + 2\mathbb{C}_{422} \\
\mathbb{C}_{440}\mathbb{C}_{220} &= \mathbb{C}_{220}\mathbb{C}_{440} \\
&= 12(d-2)(d-3)\mathbb{C}_{220} + 8(d-4)\mathbb{C}_{440} - 24\mathbb{C}_{422} + \mathbb{C}_{660} + \mathbb{C}_{642} \\
\mathbb{C}_{220}\mathbb{C}_{422} &= \mathbb{C}_{422}\mathbb{C}_{220} \\
&= 4(d-2)(d-3)\mathbb{C}_{220} - 4\mathbb{C}_{440} + 4(2d-7)\mathbb{C}_{422} + 3\mathbb{C}_{444} + \mathbb{C}_{642} \\
\mathbb{C}_{220}\mathbb{C}_{660} &= \mathbb{C}_{660}\mathbb{C}_{220} \\
&= 30(d-4)(d-5)\mathbb{C}_{440} + 12(d-6)\mathbb{C}_{660} - 30\mathbb{C}_{642} + \mathbb{C}_{880} + \mathbb{C}_{862} \\
\mathbb{C}_{220}\mathbb{C}_{642} &= \mathbb{C}_{642}\mathbb{C}_{220} \\
&= 4(d-4)(d-5)\mathbb{C}_{440} + 24(d-4)(d-5)\mathbb{C}_{422} - 72\mathbb{C}_{444} - 4\mathbb{C}_{660} \\
&\quad + 2(6d-35)\mathbb{C}_{642} + \mathbb{C}_{862} + 2\mathbb{C}_{844} + 2\mathbb{C}_{664} \\
\mathbb{C}_{220}\mathbb{C}_{444} &= \mathbb{C}_{444}\mathbb{C}_{220} \\
&= 2(d-4)(d-5)\mathbb{C}_{422} + 12(d-4)\mathbb{C}_{444} - 2\mathbb{C}_{642} + \mathbb{C}_{664} \\
\mathbb{C}_{440}\mathbb{C}_{440} &= 72d(d-1)(d-2)(d-3)\mathbb{C}_{000} + 96(d-2)(d-3)(d-4)\mathbb{C}_{220} \\
&\quad + 24(3d^2 - 27d + 62)\mathbb{C}_{440} - 432\mathbb{C}_{444} + 16(d-6)\mathbb{C}_{660} + \mathbb{C}_{880} + 2\mathbb{C}_{844} \\
\mathbb{C}_{440}\mathbb{C}_{422} &= \mathbb{C}_{422}\mathbb{C}_{440} \\
&= -48(d-2)(d-3)\mathbb{C}_{220} + 24(d^2 - 13d + 37)\mathbb{C}_{422} + 144\mathbb{C}_{444} + 8(d-9)\mathbb{C}_{642} \\
&\quad + \mathbb{C}_{862} + \mathbb{C}_{664} \\
\mathbb{C}_{422}\mathbb{C}_{422} &= 12d(d-1)(d-2)(d-3)\mathbb{C}_{000} + 8(2d-7)(d-2)(d-3)\mathbb{C}_{220} \\
&\quad + 4(d^2 - 13d + 37)\mathbb{C}_{440} + 4(5d-19)(d-2)\mathbb{C}_{422} + 12(2d-17)\mathbb{C}_{444} \\
&\quad - 4\mathbb{C}_{660} + 4(d-3)\mathbb{C}_{642} + \mathbb{C}_{844} + 2\mathbb{C}_{664}
\end{aligned} \tag{A.1}$$

in addition to the trivial products

$$\mathbb{C}_{000}\mathbb{C}_{qrs} = \mathbb{C}_{qrs}\mathbb{C}_{000} = \mathbb{C}_{qrs} \tag{A.2}$$

for arbitrary q , r and s . We note the first equation of (A.1) is equivalent to (3.4). Also the order of the products of different \mathbb{C}_{qrs} produces the same expression.

References.

- [1] G.S. Bali et al (RQCD collaboration), J. High Energy Phys. **02** (2016), 070.

- [2] G.S. Bali et al (RQCD collaboration), Eur. Phys. **A55** (2019), 116.
- [3] Z.-F. Deng, C. Han, W. Wang, J. Zeng & J.-L. Zhang, J. High Energy Phys. **07** (2023), 191.
- [4] C. Han, Y. Su, W. Wang & J.-L. Zhang, J. High Energy Phys. **12** (2023), 044.
- [5] C. Han, W. Wang, J. Zeng & J.-L. Zhang, J. High Energy Phys. **07** (2024), 019.
- [6] M.-H. Chu et al (Lattice Parton Collaboration), Phys. Rev. **D111** (2025), 034510.
- [7] G.S. Bali et al (RQCD collaboration), Phys. Rev. **D111** (2025), 094517.
- [8] G.P. Lepage & S.J. Brodsky, Phys. Rev. Lett. **43** (1979), 545.
- [9] G.P. Lepage & S.J. Brodsky, Phys. Rev. **D22** (1980), 2157.
- [10] M.E. Peskin, Phys. Lett. **B88** (1979), 128.
- [11] A.A. Pivovarov & L.R. Surguladze, Nucl. Phys. **B360** (1991), 97.
- [12] S. Kränkl & A. Manashov, Phys. Lett. **B703** (2011), 519.
- [13] J.A. Gracey, J. High Energy Phys. **09** (2012), 052.
- [14] B.A. Kniehl & O.L. Veretin, Nucl. Phys. **B992** (2023), 116210.
- [15] T. Ueda, B. Ruijl & J.A.M. Vermaseren, PoS **LL2016** (2016), 070.
- [16] T. Ueda, B. Ruijl & J.A.M. Vermaseren, Comput. Phys. Commun. **253** (2020), 107198.
- [17] J.A.M. Vermaseren, math-ph/0010025.
- [18] M. Tentyukov & J.A.M. Vermaseren, Comput. Phys. Commun. **181** (2010), 1419.
- [19] C. Pica & F. Sannino, Phys. Rev. **D94** (2016), 071702.
- [20] J.A. Gracey, T.A. Ryttov & R. Shrock, Phys. Rev. **D97** (2018), 116018.
- [21] T.A. Ryttov & K. Tuominen, J. High Energy Phys. **04** (2019), 173.
- [22] D.B. Franzosi & G. Ferretti, SciPost Phys. **7** (2019), 027.
- [23] G. Cacciapaglia, C. Pica & F. Sannino, Phys. Rept. **877** (2020), 1.
- [24] E. Bennett et al, Phys. Rev. **D109** (2024), 094512.
- [25] R. Tsuji, Y. Aoki, Y. Kuramashi & E. Shintani, PoS **LATTICE2024** (2025), 435.
- [26] T. Banks & A. Zaks, Nucl. Phys. **B196** (1982), 189.
- [27] A.D. Kennedy, J. Math. Phys. **22** (1981), 1330.
- [28] A. Bondi, G. Curci, G. Paffuti & P. Rossi, Ann. Phys. **199** (1990), 268.
- [29] A.N. Vasil'ev, S.É. Derkachov & N.A. Kivel, Theor. Math. Phys. **103** (1995), 487.
- [30] A.N. Vasil'ev, M.I. Vyazovskii, S.É. Derkachov & N.A. Kivel, Theor. Math. Phys. **107** (1996), 441.
- [31] A.N. Vasil'ev, M.I. Vyazovskii, S.É. Derkachov & N.A. Kivel, Theor. Math. Phys. **107** (1996), 710.

- [32] S.A. Larin, Phys. Lett. **B303** (1993), 113.
- [33] P. Nogueira, J. Comput. Phys. **105** (1993), 279.
- [34] V.M. Braun, S.É. Derkachov & A. Manashov, Phys. Rev. Lett. **81** (1998), 2020.
- [35] S. Kränkl, Diplomarbeit University of Regensburg (2011).
- [36] L. Vecchi, Phys. Rev. **D97** (2018), 116016.
- [37] W.E. Caswell, Phys. Rev. Lett. **33** (1974), 244.
- [38] T.A. Rytov & R. Shrock, Phys. Rev. **D94** (2016), 105014.
- [39] J.A. Gracey, Data representing the main results recorded here are available from the arXiv version of this article arXiv:2510.21940 (2025).